2018 25th Congress of International Federation for Heat Treatment and Surface Engineering

11-14 September 2018 | Xi`an China

PROCEEDINGS

Organized by Chinese Heat Treatment Society（CHTS）

25th IFHTSE CONGRESS PROCEEDINGS

11-14 September 2018

Xi'an China

Chinese Heat Treatment Society

Tel：+86（0）10 6292 0613 • Email：chts@chts.org.cn • Web:www.chts.org.cn

Add: 18 Xueqing Rd.,Beijing,China

CONTENTS

Solidification and Solid State Phase Transfromation

Kinetic process of homogenization pores growth during homogenization for nickel-base single crystal superalloys

Yanbin Zhang, Lin Liu, Taiwen Huang, Hengzhi Fu
(Northwestern Polytechnical University)
linliu@nwpu.edu.cn

Abstract: Nickle based single crystal superalloys have excellent high temperature mechanical properties, corrosion-resistance and oxidation-resistance properties, thus, are widely used in advanced turbine blades. The mechanical properties of blades are sensitive to defects. With defects like micro pores, fatigue damage easily occurs under the alternate loading in long-time service. Many investigations have shown that the porosity and size of micro pores strongly influence the fatigue property, especially for homogenization pores generated by diffusion process during solution heat treatment. To reduce the homogenization pores, a lot of research work has been carried out. Hot isostatic pressing seems to be an effective way to eliminate homogenization pores. However, some researchers found out that the H-pores, eliminated by HIP, re-opened during the subsequent creep stage. The creep property thus improves little after HIP.

To study the growth kinetics model of homogenization pores, the corresponding diffusion processes during solution heat treatment have been simulated by DICTRA software. The calculated results of homogenization pores were verified by experiments. The results show that the homogenization pores increase first and then decrease during the solution heat treatment. This is due to the imbalanced cross diffusion between dendritic core and interdendritic areas. At the beginning of solution heat treatment, fast diffusion elements like Al segregated in interdendritic areas play a leading role in the diffusion process. This results in the enrichment of vacancies in interdendritic areas and the growth of homogenization pores. After a while, the elements with high diffusion coefficients become uniformity and reach their equilibria. Then the refractory elements with low diffusion coefficients play a leading role in the diffusion process. Contrary to the beginning of solution heat treatment, the vacancy annihilates. This mechanism can be utilized in adjusting the homogenization porosity. Instead of adding a process of hot isostatic pressing, prolonging solution time could reduce both porosity and segregation, which is benefit to the creep property according to former literature.

Moreover, to reduce the homogenization pores, the influence of directional solidification parameters on the homogenization pores was investigated. Two kind of directional solidification processes were used to obtain samples with different dendritic size. The results show that with the increase of the cooling rate of solidification, the dendritic size decreases from 260 μm to 83 μm and, thus, the diffusion distance between dendrites becomes shorter. Diffusion rate of elements between dendritic structures increases which balances the cross diffusion between dendritic core and interdendritic areas. After solution heat treatment, the homogenization porosity decreases. The results provide a new basis for controlling homogenization pores by directional solidification and heat treatment process. Refining dendritic structure significantly reduce porosity without prolonging solution time. Furthermore, refining dendritic structure restrains the residual segregation, which is also benefit to the mechanical property.

In conclusion, the growth kinetics model of homogenization porosity has studied. The homogenization porosity increase first and then decrease during the solution heat treatment, due to the imbalanced cross diffusion between dendritic core and interdendritic areas. Moreover, with the decreases of the dendritic size, the diffusion rate increases. After the solution heat treatment, the residual segregation and homogenization porosity decreases. The results provide a new basis for controlling homogenization porosity by directional solidification and heat treatment processes.

Keywords: homogenization pores, solution heat treatment, superlloys, dendritic size

Analysis of free dendritic growth considering nonisothermal and nonisosolutal interface and relaxation effect

Shucheng Liu[1], Shu Li[2], Lihua Liu[1]
(1. Harbin Institute of Technology; 2. Harbin University of Science and Technology)
lishu@hrbust.edu.cn

Abstract: The free dendritic growth in an undercooled melt has attracted focused attention in the research of solidification experiment as well as theory in the past decades. To model free dendritic growth, three parts must be treated, including interface kinetics, thermal or solutal transport in the bulk liquid and morphological stability for the solid-liquid (S/L) interface. For the interface kinetics, Turnbull's collision-limited growth model is commonly used, for both metals and alloys, to describe an interface responce function, i.e. a relationship between the interfacial migration velocity, temperature and compositions of solid and liquid phases. To describe the thermal and solutal transport in liquid ahead of the S/L interface, the classical Fick diffusion equation or the extended hyperbolic diffusion equation was used. The first attempt was made by Ivantsov to obtain an exact solution with the assumption of isothermal and isosolutal S/L interface of a paraboloid of revolution. Based on the Ivantsov's result, a series of free dendritic growth models were proposed. In reality, the curvature and normal velocity are variable along the S/L interface under the steady state growth condition. This means that the interface is nonisothermal and nonisosolutal. Therefore, taking into account the anisotropic nature of the S/L interface is meaningful. Eliminating the isothermal and isosolutal S/L interface assumption, we have further obtained the exact solution of steady state Fick diffusion equation, previously (Acta Materialia, 83 (2015) 310-317). In that paper, however, the relaxation effect of local nonequilibrium solute diffusion in bulk liquid was not taken into account. In the present work, a more improved version of the free dendritic growth model was proposed by considering both the effect of nonisothermal and nonisosolutal nature of the S/L interface and the relaxation effect of solute diffusion. Comparative analysis on the present model and the corresponding model assuming an isothermal and isosolutal interface indicates that there is a higher interfacial temperature predicted by the present model. It is attributed to the two factors. The first is the sidewise thermal diffusion. The second is the solutal diffusion in the bulk liquid, with the boundary condition of the nonisothermal and nonisosolutal interface. It is finally concluded that the effect of the nonisothermal nature of the interface on the dendritic solidification behavior is significant and thus this effect should be taken into account in modelling free dendritic growth for binary alloys. Model test also indicates that the parameter nonisosolutal factors N_c introduced into the present model to denote the effect of nonisosolutal interface decreases from 1 and then increases to 1 with increasing bath undercooling. However, the maximum deviation of the value N_c from 1 is very small. Therefore, the effect of the nonisosolutal nature of the interface can be neglected in modeling free dendritic growth. In order to verify the present model, appling to the $Cu_{70}Ni_{30}$ alloy, an agreement of the model predictions with the available experiment data was obtained, due to the consideration of the relaxation effect of local nonequilibrium solute diffusion in bulk liquid.

Keywords: modeling, dendritic solidification, nonisothermal and nonisosolutal interface, relaxation effect, alloys

Modeling concentrated multi-component dendrite growth in vertical twin-roll casting

Yubing Zhang, Feng Liu
(State Key Laboratory of Solidification Processing, Northwestern Polytechnical University, Xi'an, China)
liufeng@nwpu.edu.cn

Abstract: Dendrite growth is an important stage in the solidification process of vertical twin-roll casting. The steady-state rolls counter-rotate at a given velocity and nuclei continually form at the meniscus region of each roll with further dendrite growth generating two solid shells that thicken as they move with the rolls. As the shells approach roll bite point, their dendrite networks interact and combine to form the final solidified strip. Therefore, the optimum location of the roll bite point position can influence the microstructure and property of the solidifying strip that form on the rolls. Combining the geometrical height of roll bite point position with dendrite growth was first introduced to the vertical twin-roll casting. Most theoretical work on dendrite growth has focused on under-cooled dilute binary alloys, while the vertical twin-roll casting is overheated multi-component systems. Therefore, we need to consider the characteristics of twin-roll casting and establish a dendrite growth model suitable for such solidification conditions. Due to sub-rapid directional solidification rate, solidification is lower than under cooled condition, thus the solute diffusion in the bulk liquid is under the local equilibrium condition. The marginal stability criterion, according to the solidification conditions, can be simplified further. For example, the heat diffusion in the solid can be neglected for free dendrite growth, i.e., Gs=0. For constrained dendrite growth in sub-rapid directional solidification, it is reasonable to assume and Gl=0 and $\xi_s \approx 1$. During solidification, latent heat is also released at the moving solid-liquid interface with the major impediments to its removal being the solidifying metal itself, the metal/mould interface and the mould. At the metal/mould interface, there are regions of solid-solid contact of area, and no direct contact of area which may originate from an gas film at the meniscus between the solidifying strip and the moving rolls. By incorporating the local equilibrium effects both at the interface and in the bulk liquid, positive temperature gradient, diffusional interaction and the metal/mould interface, a model was developed for constrained dendrite growth in multi-component alloys. Coupling the geometric model with the dendrite growth model, the twin roll bite point position can be determined quantitatively with a certain processing parameters. The model as guidance for vertical twin roll casting reassesses our understanding of the relationship between? height of roll bite point position, microstructure and properties.

Keywords: dendrite growth, sub-rapid directional solidification, vertical twin-roll casting, roll bite point position

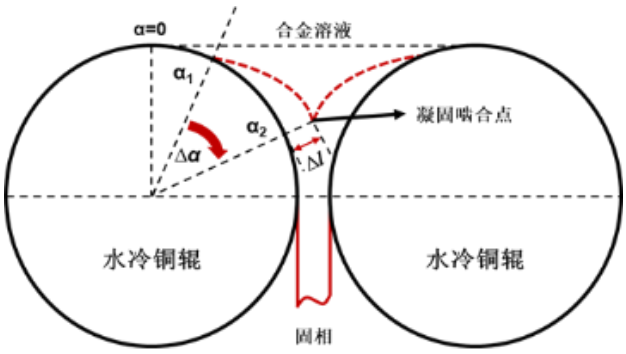

Fig.1

Centerline inhomogeneity of flat products

M. Réger
(Óbuda University)
reger@uni-obuda.hu

Abstract: Defect free casting requires an excellent accordance between steel properties being cast and the technological parameters, especially from the aspect of inner quality and homogeneity of cast products. One of the most unpredictable defects of cast slabs is the centerline segregation. The centerline segregation in slabs develops in a complex way; it is connected partly to the macro segregation and partly to the shrinkage of solidifying melt. Because of these processes, the centerline segregated part of the slab will have a different chemical composition compared to the average composition and/or it will contain shrinkage holes. After the solidification process during hot rolling the complex shaped interdendritic holes will be closed as a function of strains. The difference in chemical composition will remain even after the slab has spent several hours at over 1000 ℃ in the soaking furnace before hot rolling. Heavy plates with centerline segregation will contain, depending on the solidification and technological parameters, a middle part with a chemical composition dissimilar to the average (i.e. in case of St52 grade the segregated area can be characterized by a carbon content of 0.3-0.5wt% and manganese content of 1.7-1.9wt%). According to the industrial experiences, the segregation level (including the carbon content) can hardly be decreased by heat treatment.

The centerline inhomogeneity frozen in the slab structure can have a detrimental effect on the properties of semi or final hot rolled products, i.e. some remaining forms of this casting defect can be identified even in hot rolled strips. During hot rolling the centerline segregation pattern will become thinner and will be stretched, but it can also be detected in the middle part of heavy plates and coils. The modification of centerline segregation pattern was physically and mathematically modeled. Diffusional calculations proved the governing role of carbon activity on the homogenization process, which is also influenced by the distribution of alloying elements. The cross-effect between carbon and alloying elements (i.e. manganese) in the diffusional homogenization process of austenite can be described by the presented method. The calculation results are in good accordance both with the measured hardness distributions and with the industrial experiences concerning centerline segregation. Manganese seems to have a double role in the stability of centerline segregation. It diffuses very slowly, so there is no chance for manganese homogenization under industrial circumstances and this must result in a higher carbon content in the centerline area than the average carbon content according to the described mechanism. On the other hand, during the transformation processes manganese enhances the formation of harder microstructural constituents with lower plasticity like pearlite, bainite and martensite, which, in general, are harmful for the quality of the product.

Keywords: centerline segregation, inner quality, homogeneity

Thermal stability of directionally solidified NiAl-Cr(Mo) eutectic lamellar structure

Lei Wang[1], Jun Shen[2], Guojun Zhang[1], Hengzhi Fu[2]
(1. School of Materials Science and Engineering, Xi'an University of Technology, Xi'an, China;
2. State Key Laboratory of Solidification Processing, Northwestern Poly technical University, Xi'an, China)
wang_lei@xaut.edu.cn

Abstract: NiAl-Cr(Mo) eutectic alloy possesses a vast application prospect (like aeroengine hot end components) due to some advantages, such as high melting temperature, relatively low density, good thermal conductivity and excellent oxidation resistance. It is necessary to investigate the thermal stability of NiAl-Cr(Mo) eutectic lamellar structure for the application in the field of aeroengine. The specimens are prepared by directional solidification at various withdrawal rates (2.5-160 μm/s), and then are heat-treated at 900-1100 ℃/400 h. Two etching ways are adopted to characterize the microstructural evolution, like mild etching and deep etching. The mild etching result shows that the lamellar structure has no significant change after various temperatures (900-1100 ℃) at 2.5 μm/s (interlamellar spacing, 3.7 μm). With increasing the withdrawal rates (decreasing the interlamellar spacing), the degradation of lamellar structure occurs at the present experimental temperature (900-1100 ℃), such as coarsening, migration, pinching off, even spheroidization of Cr(Mo) phase. The deep etching and the observation of inclining 45 °to growth direction reveal that the pinching off and spheroidization observed by mild etching (Fig.1b) is not true. Actually, the local dissolution (U type groove in Fig.1c) and the cylinderization (Cylinder in Fig.1c) occur in Cr(Mo) phase. It is found that the lamellar degradation generally occurs due to the presence of structural defects, like lamellar terminations and ledges. Preliminary analysis suggests that the decrease of microstructural stability is attributed to the larger total interfacial free energy per unit volume at higher withdrawal rates (smaller interlamellar spacing).

Keywords: NiAl-Cr(Mo) eutectic alloy, directional solidification, thermal stability of lamellar structure

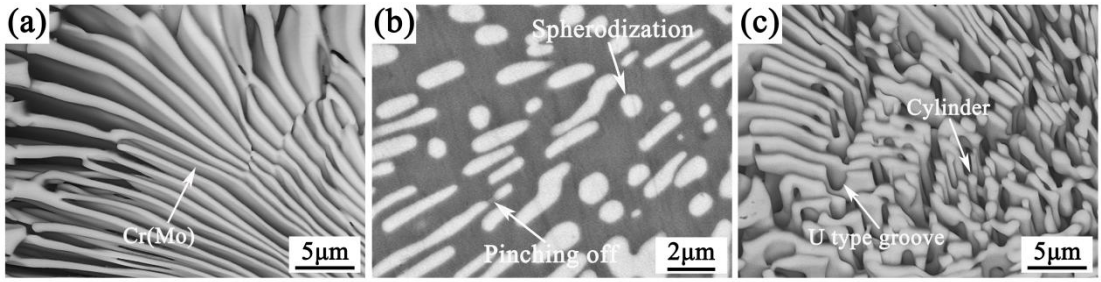

Fig.1 Microstructural evolution of directionally solidified NiAl-Cr(Mo) eutectic alloy at 160 μm/s before and after 1100 ℃/400 h: (a) deep-etched microstructure of cast alloy (inclining 45 °to growth direction), (b) mild-etched microstructure of heat-treated alloy (transverse) and (c) deep-etched microstructure of heat-treated alloy (inclining 45 °to growth direction)

Mechanism of competitive converging grains growth during directional solidification of Ni-based bi-crystal superalloys

Songsong Hu, Lin Liu, Qiangwei Cui, Wenchao Yang, Taiwen Huang, Jun Zhang
(State Key Laboratory of Solidification Processing, Northwestern Polytechnical University)
husong12030@163.com

Abstract: As a key factor for the preparation of Ni-based single crystal turbine blades, the competitive growth during directional solidification becomes a hot spot due to the discovery of some experimental results inconsistent with the classical Walton-Chalmers model. In order to explore the mechanism of competitive converging grains growth, the microstructure evolution and the dendrite spacing distribution were characterized in Ni-based bi-crystal superalloys with different withdrawal rates and crystallographic orientation.

A third-generation Ni-based single crystal superalloy DD33 was used in this study for directional solidification bi-crystal experiments with thermal gradient of ~170 K/cm. The <001> direction of favorable oriented (FO) grain was parallel to the thermal gradient, meanwhile, the <001> direction of unfavorable oriented (FO) grain deviated thermal gradient from 20 °. The metallographic microstructures were observed by Optical Microscopy (DM-4000 M; Leica, Berlin, Germany). A professional image analysis software (Image Pro Plus 6.0) was used to measure grain area. The minimum spanning tree method was used for statistics of dendrite spacing distribution based on identification of the centers of dendrites from the transverse microstructure.

The results showed that the withdrawal rate strongly affected the overgrowth for converging dendrites. At low withdrawal rate, the UO grain could overgrow the FO grain while the FO dendrite overgrew the UO dendrites at high withdrawal rate. There existed a needed critical withdrawal rate for bi-crystals coexisted which was affected obviously by the secondary orientation of FO grain with respect to the grain boundary. The needed lowest critical withdrawal rate (75 μm/s) was obtained when the secondary dendrite orientation (SDO) was perpendicular to the grain boundary of bi-crystal samples. With increase of SDO, the needed critical withdrawal rate generally increased. When the SDO was increased to 45 °, the needed critical withdrawal rate for competitive growth was largest of 300 μm/s.

Competitive growth actually took place in three-dimensional space, the insertion between UO dendrites and FO dendrites and the corresponding lateral motion resulted in the dendrite spacing at the grain boundary deviating from the stable range. As a selection criterion, the relative spacing at the grain boundary with respect to the spacing inside the FO grain had been identified. In particular the FO grain had been overgrown if its minimum spacing at the grain boundary had been smaller than the minimum spacing inside the FO grain. On the contrary the FO grain overgrew the UO grain if the maximum dendrite spacing at the grain boundary was larger than that inside the FO grain. Furthermore, the overgrowth speed was correlation with the ratio between the number of dendrite spacings at the grain boundary out of the stable range inside the FO grain and the total number of dendrite spacings at the grain boundary.

The mechanism of competitive converging grains growth was experimentally validated that the dendrite spacing was adjusted to a stable range by the development of new FO dendrites or the elimination of existing FO dendrites.

Keywords: competitive growth, withdrawal rate, crystallographic orientation, directional solidification, Ni-based superalloys

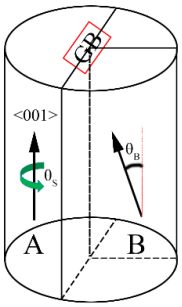

Fig.1

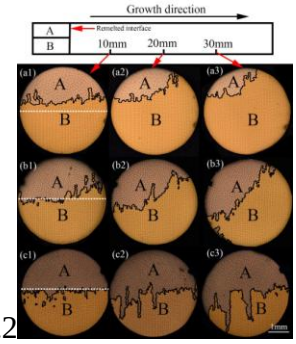

Fig.2

Fig.1 Schematic diagram showing the relationship between the FO seed A and UO seed B

Fig.2 Microstructure evolution of the bi-crystal with different withdrawal rates in Case 2: (a1-a3) 50 μm/s; (b1-b3) 100 μm/s; (c1-c3) 200 μm/s

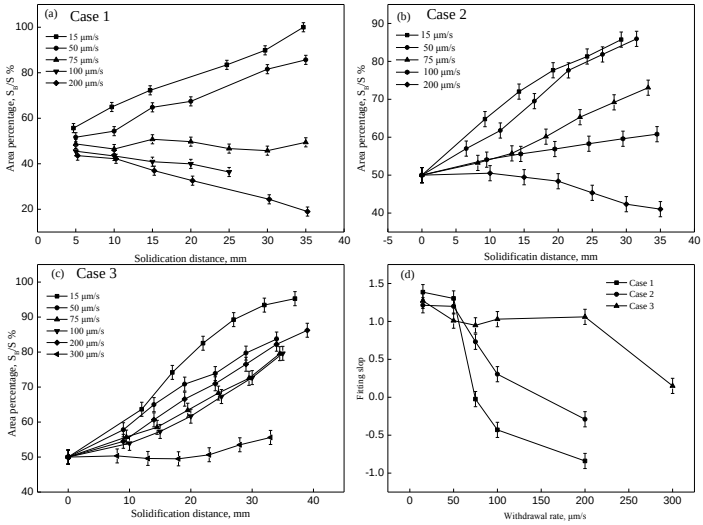

Fig.3 The variation of SB/S with solidification distance in different withdrawal rates, and the fitting slope of Case 1, Case 2 and Case 3

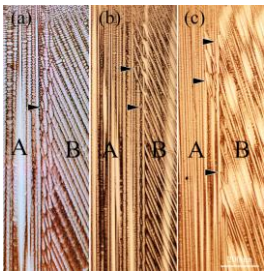

Fig.4 The quenched microstructure of longitudinal section with different second dendrite direction at withdrawal rat 100μm/s: (a) Case 1; (b) Case 2; (c) Case 3

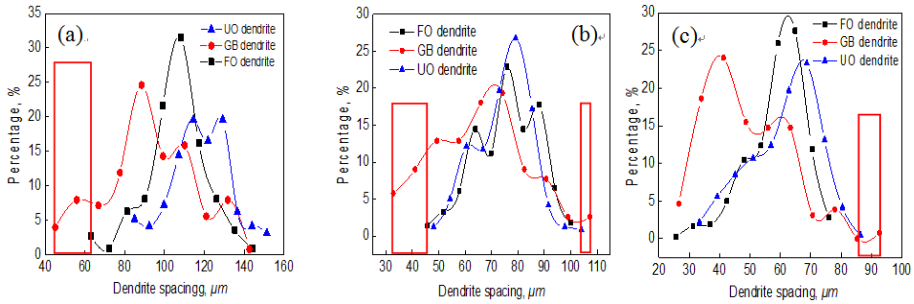

Fig.5 The frequency distribution of dendrite spacing in Case 2 at withdrawal rate (a) 50 μm/s; (b) 100 μm/s; (c) 200 μm/s

In-situ TEM study of interface migration associated with the growth of austenite precipitates

Juan Du[1], Wenzheng Zhang[1], Frédéric Mompiou[2], Zhipeng Sun[1]
(1. Tsinghua University; 2. CEMES-CNRS)
zhangwz@tsinghua.edu.cn

Abstract: Many metallic materials are strengthened by precipitates generated from solid-state phase transformation. Since the interfaces are the front of the transformation, it is of great importance to reveal the details of interface migration for a comprehensive understanding of the overall microstructure evolution of precipitates. In this report, we studied the migration behaviors of interfaces between austenite precipitate and ferrite matrix in a duplex stainless steel (DSS), together with the crystallographic features of austenite precipitates by using in-situ transmission electron microscopy (TEM). The alloy used in the present work is a commercial DSS with the composition of Fe-24.9Cr7.0Ni-3.1Mo (wt%). The as-prepared TEM foils contain either full ferrite phase or ferrite plus few pre-formed austenite, and then were heated to 700-950 ℃ by in-situ TEM equipped with heating holder. During in-situ heating, the transformation occurs either by pre-existing interfaces between austenite and ferrite matrix or by nucleation and growth of fresh austenite. The migration behavior of pre-existing interface depends significantly on the sectioning effect of the foil relative to the long axis of rod-shaped or lath-shaped austenite precipitates. The fresh austenite also exhibit an elongated morphology, but with different crystallography compared with austenite formed in bulk materials. The crystallographic features of the fresh austenite formed during in-situ heating were characterized quantitatively after cooling. Three kinds of orientation relationships (ORs) between the fresh austenite and ferrite phases have been observed, i.e. the near K-S, the near N-W and the near Pitsch OR. The long axis of fresh austenite almost invariably lies in the TEM foil surface, with a pair of near parallel habit planes passing through the foil thickness and nearly normal to the foil surface. These results show that the orientation of TEM foil exerts a significant influence on the preferential crystallography of austenite precipitates. Based on the O-line condition and the interfacial energy calculated by molecular statics, the crystallographic features of austenite precipitated in thin TEM foil were well explained by applying the criterion of minimum interfacial energy for the habit plane. During in-situ heating, the interface motion is usually accompanied with the emission of dislocations from the tip or the habit plane of fresh austenite precipitate to ferrite matrix. Besides real-time observations, the Burger vector and possible slip planes of emitted dislocations are quantitatively characterized. These experimental results verify directly that dislocation emission assists the growth of austenite precipitate. Fresh austenite precipitates with the above three kinds of OR show distinct Burgers vector and slip planes of dislocations emitted from the tip. The in-situ TEM results and theoretical calculations show that the dislocations emitted from the habit plane have the same Burgers vector with interfacial dislocations in the habit plane, implying that the dislocation emission from the habit plane is associated with the migration of interfacial dislocations.

Keywords: interface migration, in-situ TEM, precipitation crystallography, austenite precipitates

On the mechanism of nano-scale transformation twinning formation in high strength pipeline steels

Jiming Zhang[1,2], Yanshan Zhu[1], Han Ma[1], Ping Du[1], Jinbo Qu[1]
(1. Institute of Research of Iron and Steel, Shasteel, Zhangjigang, China;
2. State Key Laboratory for Performance and Structural Safety of Oil Industry Equipment Materials, Tubular Goods Research Institute of CNPC, Xi'an, China)
jiming_zhang@126.com

Abstract: A nano-scale transformation twinning (NST) was found in the X80 to X100 three fine-grained high strength pipelines. The microstructure and formation mechanism of the NSTs were characterized by a field emission transmission electron microscopy (TEM). The results showed that the NSTs were nucleated on the grain boundaries (G-Bs) and G-Bs junctions via the emission of Shockley partial dislocation from G-Bs and G-B junctions in the pipelines during the austenite to ferrite phase transformation and extended into the interior of the grains (Fig.1). Most of the NSTs displayed existence of groups of twins. The width of twinning in the groups of twins was less than five nanometers. These NSTs not passed through the entire grains but terminated the interior of grains. The dislocation intensity the grain boundary near the NSTs decreased greatly after NSTs generated.

Keywords: transformation twinning, Shockley partial dislocation, grain boundary, pipeline steel, TEM

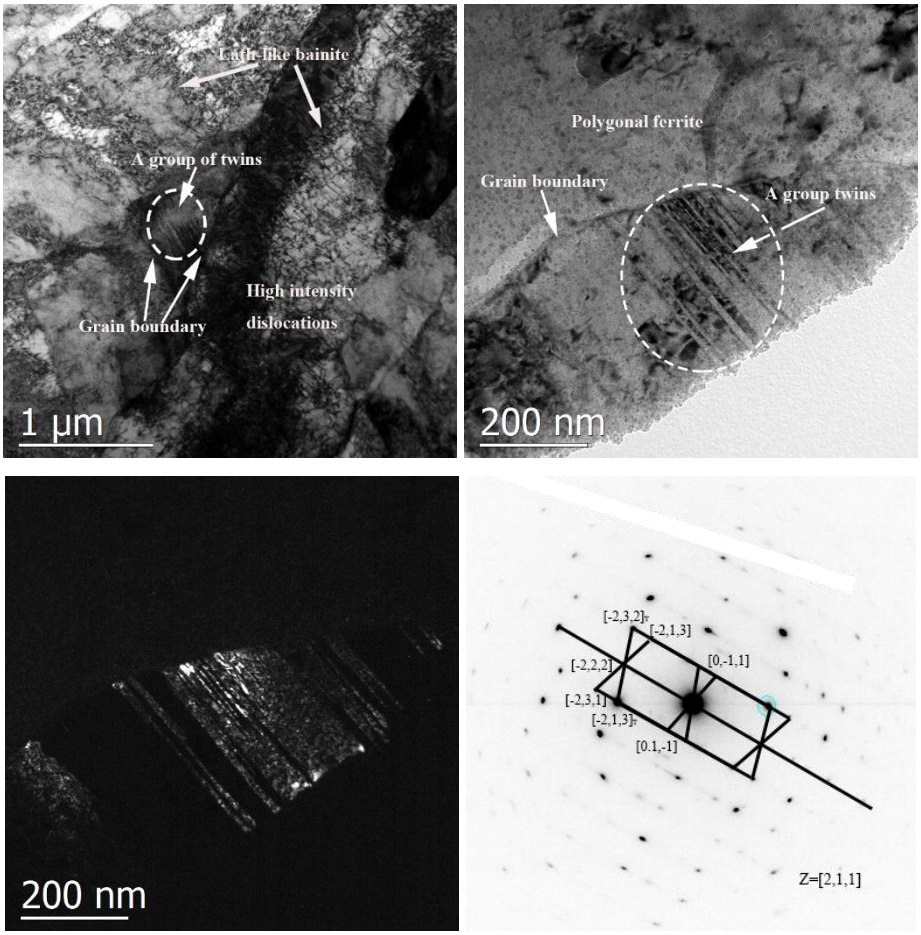

Fig.1 TEM transformation twinning images in X100 pipeline steel , (a) and (b) bright-fields micrographs of groups of twins in the white circle, and (c) dark-field micrograph of twins and (d) corresponding SAD pattern with a zone axis [211] (The black arrow in the circle indicated the direction of twinning growth)

The influence of hydrostatic pressure on shear-type austenite revision transformation

Yucong Hua, Feng Liu
(State Key Laboratory of Solidification Processing, Northwestern Polytechnical University)
liufeng@nwpu.edu.cn

Abstract: With abundant phase transformation behaviors and excellent properties, steels are widely used in modern society. According to the idea that 'phase transformation determines phases and phases determine properties', it is important to fully understand and utilize the phase transformation in steels. Austenite reversion transformation (ART) is an important phase transformation in the preparation of advanced steels, which directly manipulates the composition, morphology and distribution of austenite in steels, and thus influences the properties of steels. So, it is of great significance to study the ART.

There are now few studies on ART. Some experiments concentrated on the influence of experimental parameters on the phase transformation behavior under the condition of continuous heating or isothermal process. It is found that the phase transformation mechanisms are affected by the continuous heating rate and temperature of isothermal. The partitionless (shear-type) phase transformation occurs when the atomic migration is mild, and the needle-like reversion austenite is generated between the martensite lathes. The diffusion-type phase transformation occurs at a higher atomic mobility, and massive reversion austenite is formed at the original austenite grain boundaries. However, the mechanism of phase transformation is not deeply understood. Other experiments focused on process control to manipulate ART, which aims to improve the material properties.

The theoretical researches of ART mechanism are mainly based on classical thermodynamics models or commercial software. These works also found that there are different mechanisms under different conditions, corresponding with different ART microstructures. These researches mainly focused on the diffusion-type ART, while only a little attention was paid to the shear-type ART. Existing researches of shear-type ART mainly followed the idea of the phenomenological model, which means that thermodynamics, kinetics and crystallography are relatively independent.

In this paper, the shear-type ART is studied. Generally, carbon is retained in the newly formed lattice because the speed of transformation is too fast, which causes great distortion. The huge internal stress caused by the distortion is the main reason of the large number of crystal defects such as dislocations, twining and layer faults in the martensite phases. Taking lath martensite as an example, it was found that martensite lath was separated by continuous and highly deformed residual austenite films. The results of experimental observations show that there is a large stress between the martensite lath, which is the surrounding environment for ART. Other experimental observations also show that austenite tends to be stabilized under the condition of large ambient pressure. Based on the Mart-MIS path of the metastable intermediate state (MIS) crystallography model brought about by Xie Zhang et al, first principle calculation was conducted to figure out the influence of hydrostatic pressure on shear-type ART. It is found that decreasing hydrostatic pressure will reduce energy barrier of ART. Besides, increasing hydrostatic pressure will promote shear-type ART, which agrees well with other researches.

Keywords: austenite reversion transformation (ART), phase transformation, twining and layer faults, martensite phases

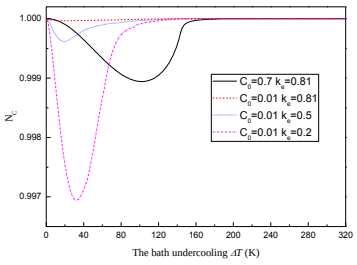

Fig.1

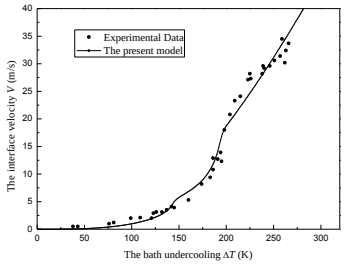

Fig.2

Study on microstructure evolution and strengthening mechanism of vanadium microalloyed dual-phase (DP) steel

Jingbin Zhang, Feng Liu
(Northwestern Polytechnical University) liufeng@nwpu.edu.cn

Abstract: For a long time, the iron and steel materials are widely used in the automotive industry. Of all the materials, the amount of steel material occupies around 70% of the total weight of a car. China's automotive industry is developing rapidly in recent years, but as the increase of car ownership in China, the pressure of environment and energy are aggravating. Under today's energy conservation and environmental protection policy advocacy, vehicle weight loss has become the focus of attention. In order to achieve the purpose of weight loss, the mechanical properties of materials must be improved so that the thickness will be reduced, and the safety of the automobiles can be guaranteed as well.

Advanced high strength steels (AHSS) are extensively used in automotive industry, such as body in white and structure automobile parts. There are three generations of AHSS-the first, the second and the third. The 1st generation AHSS are represented by IF steel, HSLA steel, DP steel and TRIP steel. The product of strength and ductility of 1st generation AHSS range from 10 to 15 GPa%. The 2nd generation AHSS are represented by TWIP steel and high manganese TRIP steel. The product of strength and ductility of 2nd generation AHSS range from 30 to 40 GPa%. The 3rd generation AHSS are represented by medium manganese steel, lightweight steel and QP steel. The product of strength and ductility of 3rd generation AHSS range from 20 to 30 GPa%. Even though the 1st generation AHSS present lower mechanical properties, it costs less than the other two generations AHSS. If we can improve the 1st generation AHSS to a higher mechanical property level by designing the chemical component and processes without increasing the cost remarkably, the AHSS will step into a new generation of high strength low cost. Consequently, we choose a typical 1st generation AHSS-DP steel to attempt to achieve high strength low cost. Dual Phase (martensite and ferrite) steel is a typical example of 1st AHSS, with martensite providing strength and ferrite providing ductility. The most advanced DP steel is DP1180 with UTS (ultimate tensile strength) > 1180MPa, uniform elongation >5%. To improve the mechanical properties of DP1180, we added vanadium to the chemical component system in order to increase UTS without decreasing elongation.

We design a new DP chemical component and the manufacture processes are reconsidered according to the chemical component. The processes include smelting, forging, hot rolling, cold rolling, isothermal precipitating, intercortical annealing and quenching. The dual phase microstructure with precipitates scattering inside is received after the quenching process. EBSD characterization shows that the primary austenite grains have two size distribution (submicron and micrometer scale). TEM characterization shows that the size distribution of VC precipitates ranges from 10 to 50 nanometer. SEM characterization shows that precipitate exists both in martensite and ferrite. The DP steel we produced presents extraordinary tensile mechanical properties with UTS>1300 MPa, YS>1000 MPa, UE (uniform elogation)>5%, TE (total elogation)>9%. The DP steel we produced satisfies the mechanical property demand of 1300 MPa DP steel.

Keywords: vanadium-microalloying, dual-phase steel, vanadium carbide, reverse transformation, intercritical annealing

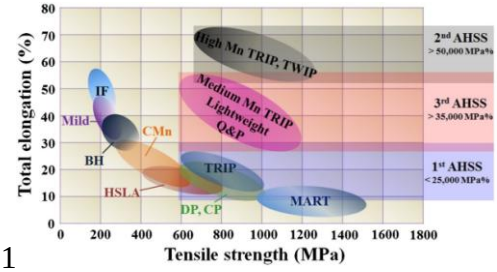

Fig.1

Analysis of the effect of alloying elements on the microcosmic thermodynamics and kinetics of martensite transformation based on ab initio simulation in steel

Tianle Wang, Feng Liu
(State Key Laboratory of Solidification Processing, Northwestern Polytechnical University, Xi'an, China)
liufeng@nwpu.edu.cn

Abstract: Martensite transformation is a key part of heat treatment principle in steel. Since the French scholar Osmond named the quenched steel as martensite in 1895, people started studying the thermodynamics, kinetics, crystallography, nucleation and growth mechanism of martensitic transformation. The characteristics of different alloying steels in martensitic transformation are often different, with different Ms temperature, nucleation rates and orientation relationships, etc. However, due to the fact that experimental-based phase transition studies are too "macro" to capture the microscopic details of the near-sonic transition of martensite, the understanding of the microscopic transformation mechanism of martensitic transformation still remains inadequate. For thermodynamics and kinetics characteristics of the martensitic transformation exhibited, we cannot give an explanation based on the microscopic nature of the phase transition.

With the development of computational materials science and the emergence of high-performance computers, it is expected that theoretical analysis methods will be used to explain some experimental phenomena from a more rational perspective. The first-principle based on quantum theory is a method for studying the structure and properties of materials at the nanoscopic scale. Because it does not depend on any empirical parameters, it is increasingly used in various materials researching process. In this paper, first principle is used to study the microscopic thermaldynamics and kinetics characteristics of martensitic transformation in different alloys in steel. It is expected that starting from the microscopic atomic transformation path, the thermaldynamics and kinetics effects of different alloying elements on the transformation path will be revealed, and it can provide evidences for some experimental phenomena. However, due to the complex phase transformation in steel compared to other alloys, the calculation considering finite temperature, magnetism, and complex components is currently very difficult, requiring long-term exploration to solve this problem. Therefore, the influence of temperature and magnetism is neglected in the study of this paper. The effect of each element on the microcosmic mechanism of phase transformation is preliminarily calculated, which will pave the way for the subsequent calculation with correction of temperature and magnetism in the field.

The first-principle atom-scale phase transition study used in this paper is mainly based on the traditional Bogers-Bugers crystallographic model and the MIS (metastable intermediate structure) crystallographic model proposed by Xie Zhang et al. in recent years. These two models have significantly different characteristics when describing the phase transition atom path. The former is dominated by lattice shear, while the latter is dominated by the internal atom shuffle of the lattice. The microscopic martensitic transformation path was modeled by establishing 3D atomic models of BB and MIS, and a solid state nudged elastic band method (SSNEB) is used to find the phase transition minimum energy path (MEP). After finding the saddle point, the driving force and energy barrier of the phase transition are known. Finally, comparing the energy barrier calculation results under different compositional alloys to find the effect of elements on the transformation path. The main conclusions are as follows:

(1) The effect of alloying elements on the BB path is greater than that of the MIS path, showing the fluctuation of the energy change curve during the transition process.

(2) When different element X with the same atomic concentration is added to pure iron, there is a energy-barrier law appearing between different Fe-X systems: $Q_{(Fe\text{-}Mn)}>Q_{(Fe\text{-}Cr)}>Q_{(Fe\text{-}Ni)}\approx Q_{(Fe\text{-}Si)}>Q_{(Fe\text{-}Cu)}$. The schematic diagram of the MEP calculation results in the MIS and BB paths is shown in Fig.1. In the MIS path and the BB path, the law of the energy barrier size exists, and within the scope of the studied composition, the variation of the concentration of element X remains basically unchanged. The law of the energy barrier exists both in the MIS path and the BB path, and it remains nearly unchanged within the scope of the studied composition with the variation of the concentration of element X. The energy barrier for the addition of interstitial atom C is greater than the energy barrier for addition of the metathesis atom (except Mn).

(3) The traditional double shear BB path and the MIS path can be coordinated and unified under the same alloy system. With the change of the element concentration X, the relative sizes of transition energy barriers of the two paths may change. So that in different situations, the actual transition is more inclined to follow one of the paths with the lower energy barrier.

(4) The calculation results after adding 3d transition metal element in pure iron show that: [1] There is a certain correlation between the size of the transition energy barrier and the number of valence electrons; [2] The influence of the 3d transition metal elements on the stacking fault energy is opposite to on the α martensite transformation energy barrier. If the stacking fault energy is increased with the adding of element, the α transformation energy barrier will be reduced, which revealing the role of element in the emerging of ε martensite and α martensite in the phase transition process.

(5) In the same Fe-X system, with the change of X concentration, element X has a different effect on the transition energy barrier in different composition ranges, and the energy barrier does not change monotonically with the increase of concentration. In a compositional interval with monotonically energy barrier changing, a trade-off relationship is found between the transitional driving force and energy barrier, which indicating the interrelationship between thermodynamics and kinetics.

The innovation of this paper is that: On the one hand, the BB double shear model is applied to the first principle researching of martensitic phase transition at the first time, and providing new ideas for the sthdy of the microscopic mechanism of martensitic transformation by simulating MIS and BB microscopic transition paths. On the other hand, the above conclusions are the summary of the calculation results, and they are also not mentioned by the predecessors. It is a new study direction worthy of future research and is of great significance for revealing the microscopic mechanism of martensitic transformation.

Keywords: martensite, crystallographic model, ab-initio calculation, NEB, energy barrier

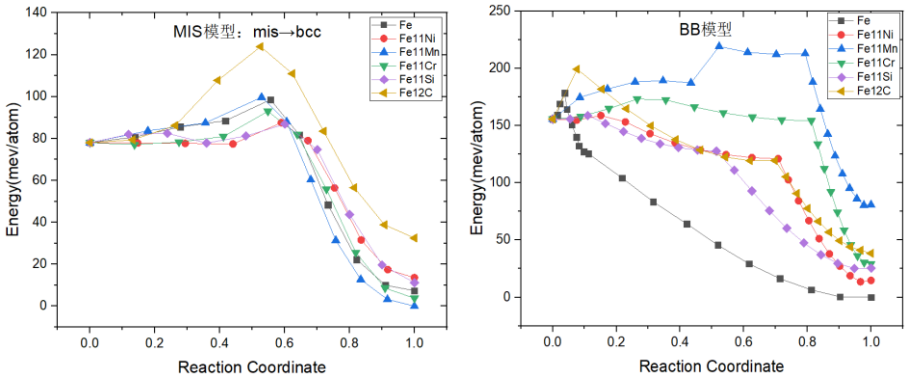

Fig.1

Microstructure of strain induced martensite in high carbon steel

Yulin Chen, Xinqing Zhao
(Beihang University)
xinqing@buaa.edu.cn

Abstract: The martensites in quenched carbon steels have been considered a carbon supersaturated homogeneous solutions until more recently transmission electron microscopy observations indicate that the martensites are composed of α-Fe and hexagonal phase. As is well known, martensite in carbon steels can be obtained by quenching or by stress/strain. However, it has yet to realize that whether the strain induced martensite possess uniformed structure or not. In the present study a metastable austenitic steel is employed to obtain strain induced martensite in high carbon steel by tensile deformation, and the microstructure of the stain induced martensite was intensively characterized by high resolution transmission electron microscopy. It was indicated that the microstructure of strain induced martensite is composed of ultrafine twins and dispersed high-density nanoscaled ω particles embedded in twin boundaries. Its formation was mainly attributed to the shear deformation on {112} planes in α-Fe. These findings not only represent the microstructure of strain induced martensite, but also provide new insight into the understanding of the design of the mechanical properties of martensite in ferrous alloys.

Keywords: strain induced martensite, microstructure

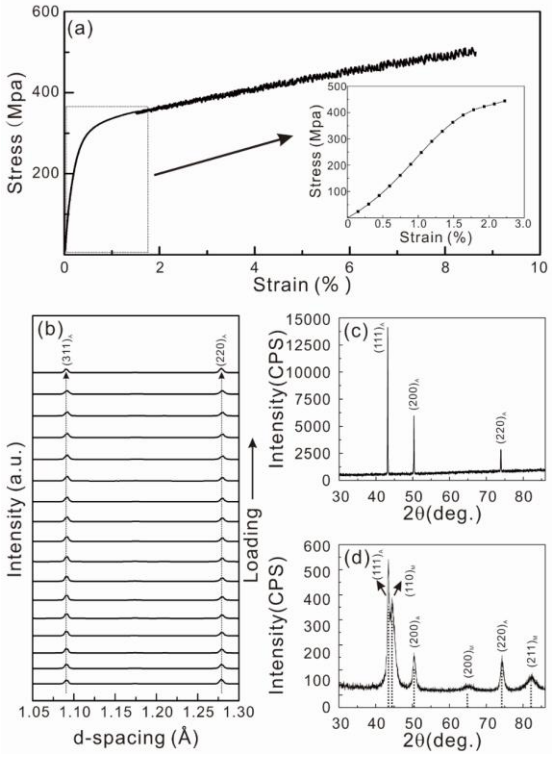

Fig.1

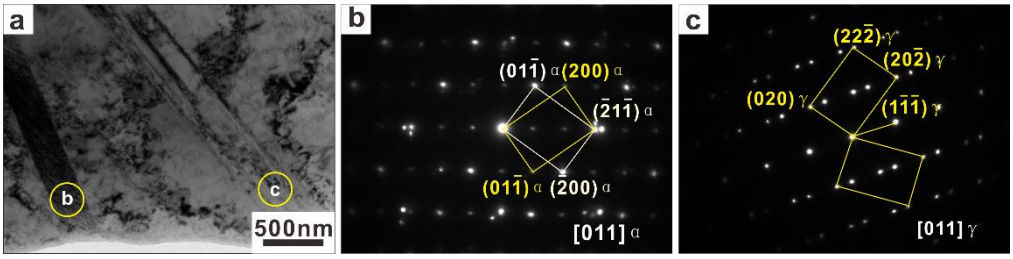

Fig.2

Numerical simulation of hydrogen diffusion behaviors in dual phase steel

Bangshu Yang[1], Lin Cheng[1], Xian Zhang[1], Jing Liu[1], Feng Hu[2], Kaiming Wu[1]
(1. Wuhan University of Science and Technology; 2. Nanjing Iron & Steel United Co., Ltd.)
chenglin@wust.edu.cn

Abstract: Hydrogen embrittlement often occurs without obvious signs, which is extremely harmful. Hydrogen diffusion and trapping behaviors within the metallic materials, which determine the hydrogen amount absorbed from the environment and hydrogen distribution in the microstructure, are the fundamental factors in predicting hydrogen embrittlement susceptibility. Multiple-phase combination is an effective design to obtain advanced high-strength steels, such as the steels with ultra-fine bainite or martensite as the matrix coupled with retained austenite. Hydrogen diffusion mechanism in such two-phase steels is one of the two outstanding challenges in hydrogen diffusion modelling because of the effects of retained austenite acting as hydrogen trapping sites due to its high hydrogen solubility and slow diffusivity as well as the effects of the phase interfaces between retained austenite and the matrix, etc. In present study, the effects of the austenite/ferrite interface on hydrogen diffusion behaviors were numerically studied.

Keywords: hydrogen diffusion, dual phase steel, numerical simulation

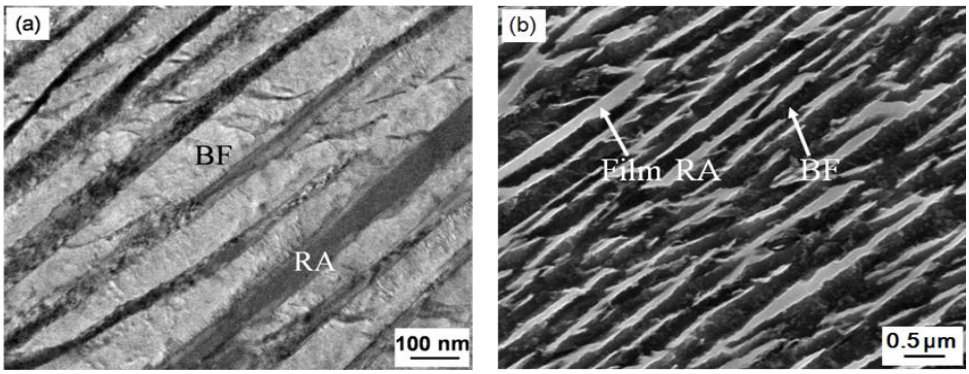

Fig.1

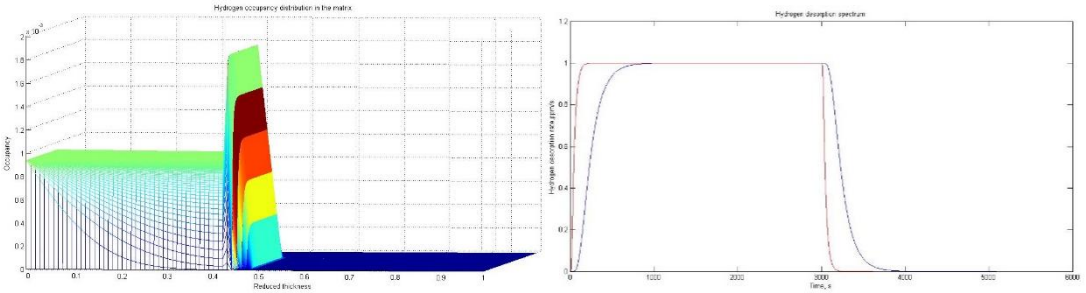

Fig.2

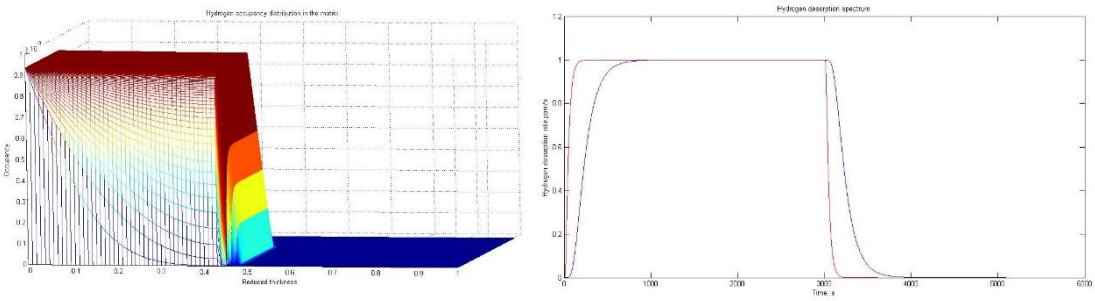

Fig.3

Influences of retained austenite on impact toughness in mediumcarbon micro/nano-structured steels

Yajie Wu[1], Feng Hu[2], Lin Cheng[1], Gang Huang[1], Kaiming Wu[1]
(1. Wuhan University of Science and Technology; 2. Nanjing Iron & Steel United Co., Ltd.)
chenglin@wust.edu.cn

Abstract: Effects of retained austenite in medium-carbon micro/nano-structured steels on impact toughness was analyzed based on the steels obtained by means of medium and low temperature bainitic transformation processes, which were dependent on the designed chemical composition. Micro-structure analysis was conducted by means of optical microscope, scanning electron microscope and transition microscope. The impact toughness analysis was conducted using Universal Testing Machine and 450J pendulum impact test machine. The results show that the impact properties of steels obtained by low temperature bainitic transformation process were significantly higher than those obtained by medium-temperature bainitic transformation process, because in medium-carbon steel retained austenite in appropriate amount was obtained within the low-temperature bainitic transformation process.

Keywords: retained austenite, micro/nano-structured steels, impact toughness

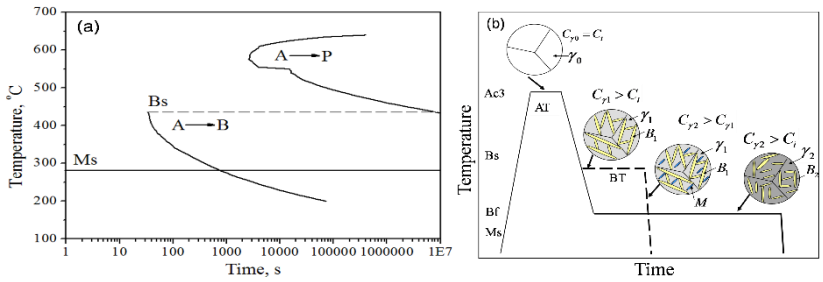

Fig.1 TTT curve(a) and schematic diagram(b) of low temperature bainite transformation

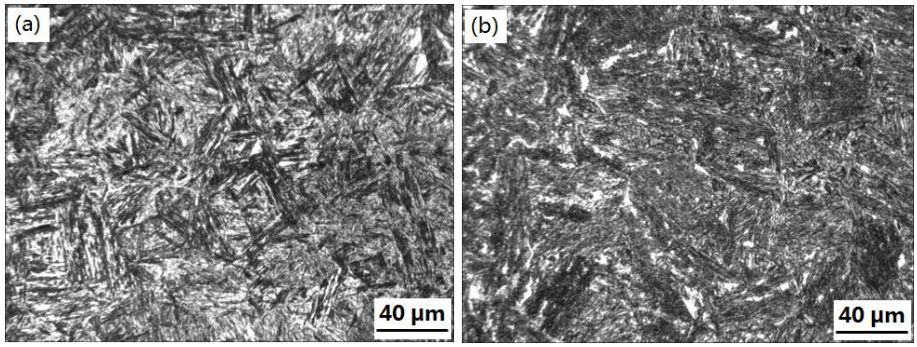

Fig.2 Optical micrographs of the investigated steel at (a) 400 ℃ for 4 hrs and (b) 320 ℃ for 24 h

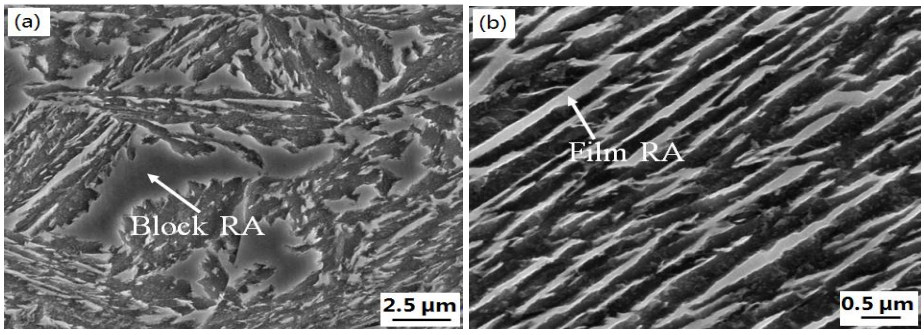

Fig.3 SEM micrographs of the investigated steel at 320 ℃ for 24 h

Effect of disorder-order transition of Al*x*CoCrFeNi high entropy alloy film on electrical resistivity temperature behavior

Chenyu Wang, Xiaona Li, Zhumin Li, Xiaotian Cheng, Qing Wang, Chuang Dong
(Key Laboratory of Materials Modification by Laser, Ion and Electron Beams,
Dalian University of Technology)
lixiaona@dlut.edu.cn

Abstract: Al*x*CoCrFeNi (*x*=0.7, 1) high entropy alloy thin films were prepared by magnetron sputtering, phase constitution, microstructure and resistivity temperature behavior were investigated. As-deposited films were formed of column grains in nano size, with duplex FCC/BCC phase. Room temperature resistivity of the films vary from 138.7-535.1 μΩ·cm, The temperature coefficient of resistivity in the range of 298-550 K is rather low and sometimes negative, drastic decrease of resistivity appears around the temperature of 550 K. To explain this kind of behavior, order-disorder transition was investigated and the similar behaviors in traditional solid solution alloys were compared, providing a more comprehensive and deeper understanding for the resistivity behavior and the characteristics of high entropy alloys solid solutions. In addition, films of these compositions can grow well on different substrates, thier material conditions are better than bulk alloys in the same composition, and more thermally stable than most of the amorphous materials, which on a certain level shows the application value of the Al*x*CoCrFeNi high entropy alloy thin films.

Keywords: high entropy alloy film, resistivity

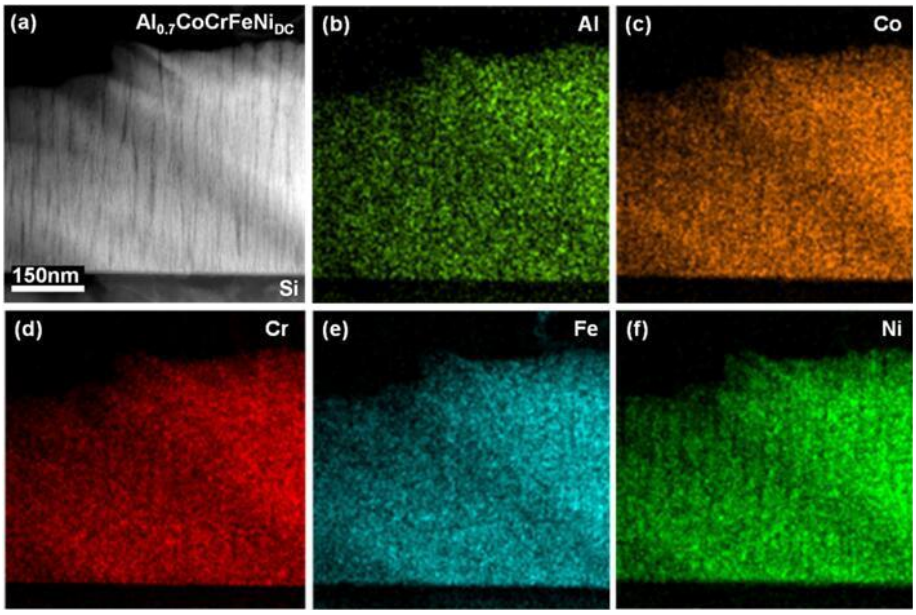

Fig.1

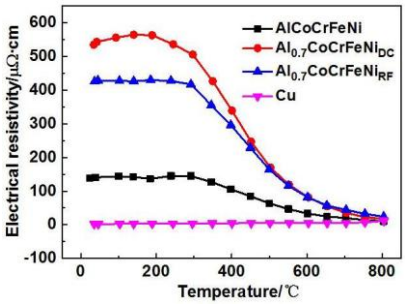

Fig.2

Research on the relationship between properties and microstructure of Cu4Ni3M (M=Al, Cr, Mo) alloys

Zhumin Li, Xiaona Li, Yuehong Zheng, Wei Sun, Xiaotian Cheng, Qingxiao Yu, Chenyu Wang, Chuang Dong
(Key Laboratory of Materials Modification by Laser, Ion and Electron Beams, Dalian University of Technology, Ministry of Education, Dalian 116024, China)
lixiaona@dlut.edu.cn

Abstract: Cu and Ni form a continuous solid solution that is face centered cubic lattice. Copper-nickel alloys have high resistance and good mechanical properties. Copper alloys with excellent properties would be obtained through suitable third element to be added to Copper-nickel alloys and control the microstructure. In this work, Cu4Ni3M (M=Al, Cr, Mo) alloys was fabricated via arc-melting and appropriate heat treatment. Three typical microstructure of copper alloys, that is γ phase +γ′ phase, modulated structure (γ_1 phase+γ_2 phase) and Ni4Mo nanophase as main strengthening phase was respectively achieved in the Cu4Ni3M (M=Al, Cr, Mo) alloys. Cu4Ni3Al alloy have a melting point is 1222.9 ℃ and a conductivity is 5.47%IACS, with a hardness is 310 HV by means of differential thermal analysis, electric conductivity test and hardness test. Cu4Ni3Al alloy demonstrate the highest melting point, the best conductivity and the supreme hardness in the Cu4Ni3M (M=Al, Cr, Mo) alloys. Meanwhile, Cu4Ni3Al alloy exhibit excellent softening resistance at high temperature during softening temperature test (200-1000 ℃). Cu4Ni3Cr alloy was softened when the temperature reach up to 1000 ℃ that mainly caused by the modulated structure coarsening and the Cr phase formed at grain boundaries. Cu4Ni3Mo alloy was softened at 400 ℃, exhibit the worst softening resistance. The studies in this paper suggest that γ′ precipitated phase have obvious advantage compared with modulated structure (γ_1 phase + γ_2 phase) and Ni4Mo nano phase as main strengthening phase on improve properties and high temperature stability of copper alloys. The copper alloys with high temperature resistance would be obtained through control the morphology and volume friction of γ′ phase.

Keywords: copper alloy, microstructure, stability, properties

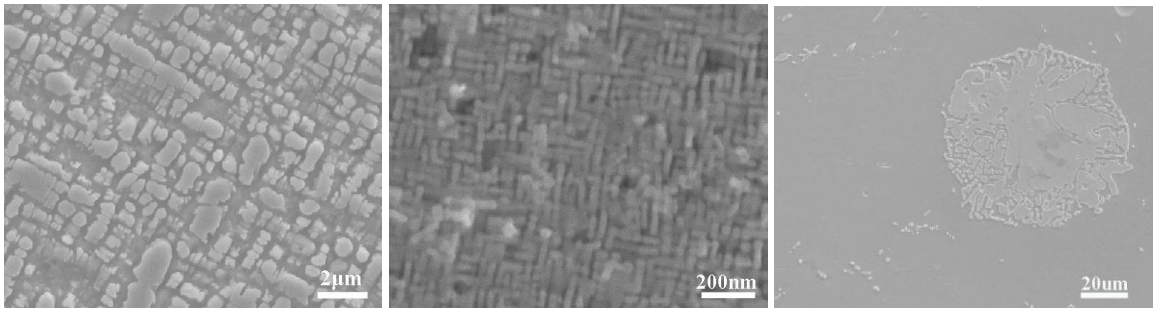

Fig. 1 the Microstructure of Cu4Ni3M (M=Al, Cr, Mo) alloys: (a) Cu4Ni3Al alloy; (b) Cu4Ni3Cr alloy; (c) Cu4Ni3Mo alloy

Pinning of coherent particles on moving plane grain boundary

Haoran Peng, Feng Liu
(State Key Laboratory of Solidification Processing, Northwestern Polytechnical University, Xi'an, China)
liufeng@nwpu.edu.cn

Abstract: Pinning effect of second-phase particle has long been demonstrated to be an extremely effective way to impede grain boundary (GB) migration to increase strength or enhance thermal stability, in particular nano-scale materials. In this paper, using Cu-Ag as a model system, the interaction between coherent nano-particle (Ag) and GB (Cu 5<310>) is studied by molecular dynamics simulations. Through measuring the GB velocity and the system energy, the maximum and averaged pinning forces of the coherent particle are calculated. On this basis, the pinning mechanism of coherent particles is discussed. Furthermore, by changing the particle parameters (e.g. particle size, particle volume fraction, particle shape) and then calculating the maximum and averaged pinning forces, the relationship between the pinning forces and the particle parameters is studied. When comparing to the prediction of the classical models, the present results show a good agreement for the maximum pinning forces, as also reported in the previous simulation.

Keywords: particle pinning, molecular dynamics

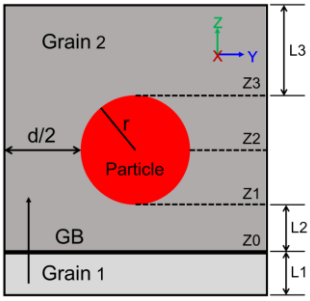

Fig.1

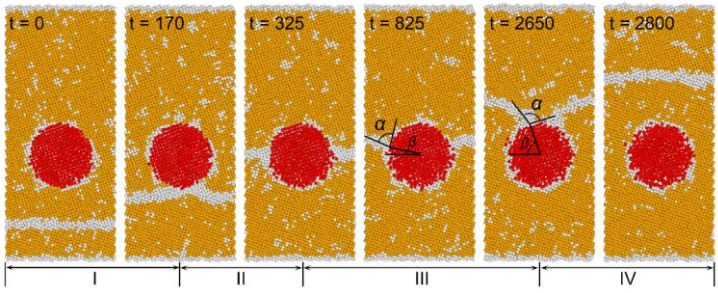

Fig.2

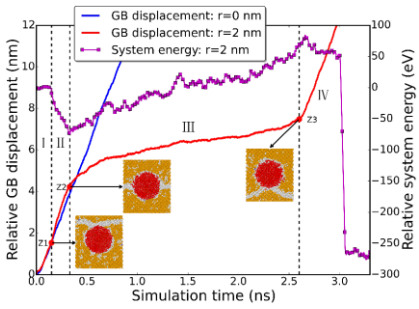

Fig.3

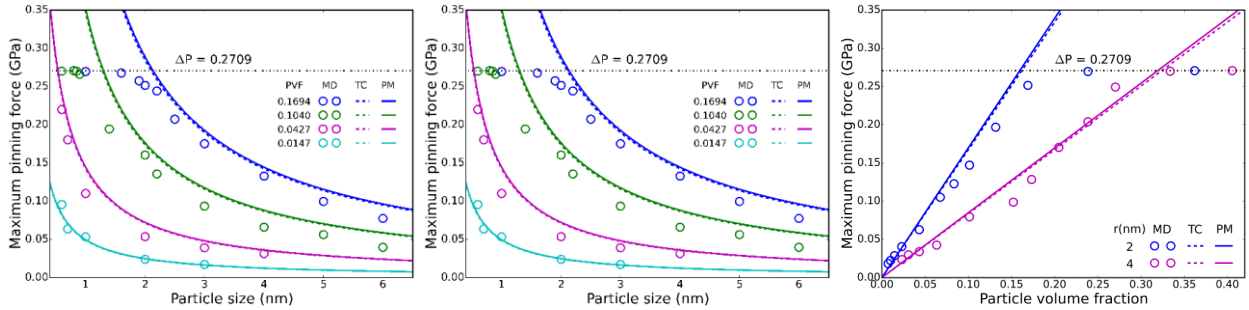

Fig.4

Multi-scale modeling of the complex microstructural evolution in structural phase transformations

Lin Zhang, Kang Wang, Feng Liu
(State Key Laboratory of Solidification Processing, Northwestern Polytechnical University, Xi'an, China)
liufeng@nwpu.edu.cn

Abstract: Microstructure in engineering alloys results from the phase transformations and determines the mechanical, physical and chemical properties of materials, and thus is of great technological importance. To understand and ultimately control the phase transformations, various theoretical models (e.g. phase field method) have been proposed over the years, which, however, are still unable to quantitatively model the microstructural evolution. Modeling the microstructural evolution in structural phase transformations remains challenging, mostly due to the competitions among potential product phases and the multi-scale nature. One of the origins to the complexity of the microstructural evolution roots in the competitions among the multiple product phases, e.g. Guinier-Preston (GP) zone, θ" and θ' in Al-Cu alloys and ferrite, bainite and martensite in steels. Other than the dilemma of multi-phase evolution, most of the previous models focus on the mesoscopic evolution with phenomenological free energy functionals, thus inevitably neglecting atomic-scale physics and introducing parameters that are difficult to be determined using atomic-scale computations (e.g. first-principles calculations, molecular dynamics).

Previous modeling of phase transformations based on the maximal entropy production principles (MEPP) generally focuses on the dissipative processes (e.g. diffusion, interface migration, etc.) and the transformation mechanism (hence the product phase) is given as a priori, thus cannot address the competitions among multiple product phases. Zhong et al., Rao et al. and Bouville et al. attempted to tackle the competitions between ferrite, bainite and martensite within the phase field framework, which, however, focused on the mesoscopic evolution and the multi-scale nature is not addressed. Actually, accurate modeling of structural phase transformations mandates the atomic-scale physics and the mesoscale thermodynamics and kinetics of the evolution. From the perspective of irreversible thermodynamics, the multiple product phases can be represented by different dissipative paths for the parent phases, each of which dissipates free energy with a different rate due to a specific mechanism of transformation. Hence, modeling the evolution of non-equilibrium phase transforming system with multiple product phases essentially reduces to the selection of evolution paths, all of which should be considered altogether. The maximal entropy production principle (MEPP) has become a natural theoretical tool for the path selection of phase transforming system.

Regarding the urgent needs in microstructural design of engineering materials, we propose an atomic-scale/mesoscopic framework that directly addresses a conception of microstructural parameters (MPs) and formulate a multi-variate Fokker-Planck type equation using the maximal entropy production principle (MEPP) with the mobilities of dissipation related to the rate coefficients for the atomic-scale processes from the variational transition state theory (VTST), such that an accurate yet practical multi-scale theory for structural transformation, free of adjustable parameters, is made possible. We focus on an arbitrary *m*-component phase transforming system with the parent phase and multiple grains of the various product phases. Applied to precipitation in Al-Cu alloys, the present model, free of adjustable parameters, predicts correct sequence of precipitation, i.e. GP zone→θ"→θ', and yields accurate precipitation kinetics for θ" and θ' as compared with previous experimental data, thus demonstrating the inherent correlation of MPs with thermodynamics and kinetics. For the complex transformations in engineering alloys, the current framework, starting from the general statistical principles and MEPP, can incorporate specific MPs for a given transformation following the same scheme.

Keywords: solid phase transformations, multi-scale, microstructural evolution

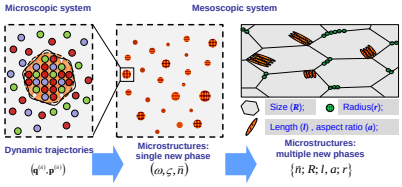

Fig.1

Characterization of TiNiCuNb shape memory alloys with excellent thermal cycling stability

Yunxiang Tong[1], Wenyin Qi[1], Li Li[1], Feng Chen[1], Bing Tian[1], Yufeng Zheng[2]
(1. Harbin Engineering University; 2. Peking University)
tongyx@hrbeu.edu.cn

Abstract: TiNi-based shape memory alloys (SMAs) have been regarded as promising actuator materials due to their large output force and large displacement. During its service life, SMAsbased actuator must be subjected to numerous thermal cycling between martensite and parent phase. This usually causes the degradation of functional properties (phase transformation temperature et al.) due to the introduction of high density dislocations, which in turn makes it difficult to accurately control the actuator. In order to achieve excellent thermal cycling stability, the conventional method is to suppress the introduction of dislocations by physical metallurgy approaches.

Very recently, the geometrically non-linear theory of martensite has been proved to be an useful method to screen for the SMAs with extreme narrow transformation hysteresis and excellent thermal cycling stability. Some SMAs have been identified as the materials with excellent thermal cycling stability. Among these alloys, Ti54Ni34Cu12 thin film is the most attractive not only for its highly stable martensitic transformation against thermal cycling, but also for its almost constant superelasticity even after 107 tensile cycles. However, when the Cu-content exceeds 10at%, the bulk alloys are too brittle to be plastically worked, which has become the main obstacle for engineering applications.

An alloying is effective in improving the cold-workability of TiNiCu-based SMAs by forming ductile phase. In order to improve the workability of Ti54Ni34Cu12 bulk alloy without obviously sacrificing thermal cycling stability, the fourth element should not influence the lattice parameters of matrix significantly and form any brittle compound with the existing element. It has been reported that Nb prefers to occupy Ti sites rather than Ni sites. The radius of Nb atom (0.143 nm) is very close to that of Ti atom (0.145 nm). The solubility of Nb in TiNiCu matrix is quite limited, for example, about 2.6at% Nb dissolve when 10at% Nb is added into Ti50Ni40Cu10 alloy. In addition, the addition of Nb favors reducing the amount of Ti_2(Ni,Cu) particles and does not form any brittle compound. Thus, it is highly expected that if Ti54Ni34Cu12 alloy is chosen as the starting material, TiNiCuNb alloys are possible to show stable martensitic transformation against thermal cycling. However, up to now, an in-depth investigation of the thermal cycling stability of TiNiCuNb alloys is still not available.

In present work,microstructure and martensitic transformation of $(Ti54Ni34Cu12)_{100-x}Nb_x$ (x=0, 6 and 10at%) was investigated. After addition of Nb, Nb-rich phase presents in the microstructure. Martensite variants are determined to be (111) type I twin and (001) compound twin. Martensitic transformation are characterized by single-step transformation. With increasing Nb content, the transformation temperature decreases.The addition of Nb enhances the cycling stability. After 500 thermal cycles, the shift of martensitic transformation temperatures of (Ti54Ni34Cu12)90Nb10 alloy is less than 0.5 K. This can be ascribed to the addition of Nb, which does not significantly decrease the crystallographic compatibility between martensite and parent phase, whereas increases the yield strength to suppress nucleation and movement of dislocations.

Keywords: shape memory alloys, martensitic transformation, microstructure, thermal cycling stability

Heterogeneous nucleation research on $YAlO_3$(001)/NbC(100) interface

Zhijun Shi, Sha Liu, Yefei Zhou, Xiaolei Xing, Changchun Zhao, Qingxiang Yang
(College of Materials Science and Engineering, Yanshan University, Qinhuangdao 066004, China)
qxyang@ysu.cn

Abstract: The microstructure, element distribution and interface condition of $YAlO_3$ and NbC in the hypereutectic Fe-Cr-C-Nb-Y_2O_3 alloy was observed by field emission scanning electron microscopy (FESEM) and transmission electron microscopy (TEM). The lattice mismatch between low index crystal surfaces of $YAlO_3$ and NbC was calculated by using the Bramfitt two-dimensional lattice mismatch theory. The work of adhesion, interfacial energy and electronic structure of the $YAlO_3$(001)-NbC(100) interface structures were calculated by utilizing the first principle method. The charge density difference, electron localization function and crystal orbits overlap population was adopted to analyze the charge transfer and bond characteristics. The SEM results show that, there is a compound contains rare earth Y element in NbC. In order to further ascertain the type of the rare earth compound, the microstructure of surfacing alloy was observed by using transmission electron microscope. The TEM results show that, the internal square particle is $YAlO_3$ and the outer annulus is NbC. And NbC grows around $YAlO_3$ and they are combined together tightly, which proved $YAlO_3$ can act as the heterogeneous nucleus of NbC experimentally. The twodimensional lattice mismatch of $YAlO_3$(001)-NbC(100) interface is 5.4%, which testifies that $YAlO_3$ can meet the lattice structure condition of being an effective heterogeneous nucleus of NbC. In all interface structures, C-O2 model has the largest work of adhesion (Wad = 6.558 J/m^2) and the work of adhesion of different interfaces has the following relationship: Wad(C-O2)>Wad(Nb-O2)> Wad(C-Y)>Wad(Nb-Y)>Wad(Nb-O1)>Wad(C-O1). While, C-Y model has the smallest interfacial energy (γ=0.54 J/m^2) and the interfacial energy$\gamma$of different interfaces has the following relationship: γ(C-Y)<γ(Nb-Y)<γ(C-O2)<γ(Nb-O2)<γ(Nb-O1)<γ(C-O1). The interface structure with the best stability is C-Y, which has the smallest interfacial energy. The chemical bonds between interface atoms are major covalent bonds and few metal bonds. The chemical bonds of Nb-Y interface and C-Y interface are both mixtures of covalent bonds and metallic ones. The chemical bonds of Nb-O2 interface and C-O2 interface are both covalent bonds. The calculation results indicate that $YAlO_3$(001) slab and NbC(100) slab can form a stable interface structure and thus $YAlO_3$ can act as an effective heterogeneous nucleus of NbC.

Keywords: Heterogeneous nucleation, YAlO3, NbC, interface properties, first principle method

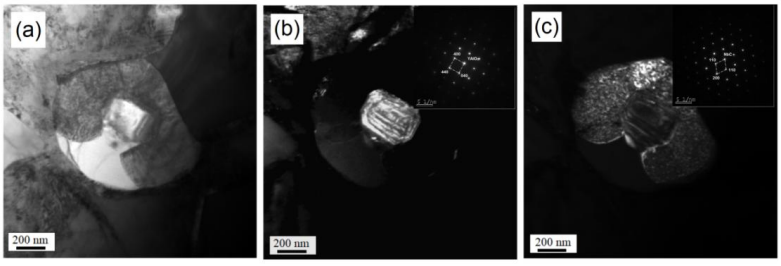

Fig.1

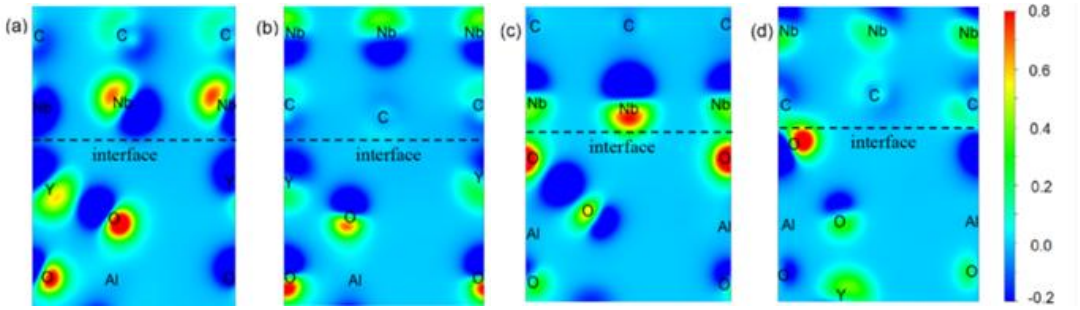

Fig.2

Heat-resistant Cux[Ni_3M1] film with '-Ni3M phase precipitation strengthening

Xiaotian Cheng, Xiaona Li, Zhumin Li, Yuehong Zheng, Qingxiao Yu, Chenyu Wang
(Key Laboratory of Materials Modification by Laser, Ion and Electron Beams, Dalian University of Technology, Ministry of Education, Dalian 116024, China)
lixiaona@dlut.edu.cn

Abstract: In many applications such as mold's internal, copper and its alloys not only pursue good conductivity and thermal conductivity, but also require its surface to have high hardness, good thermal conductivity and high temperature corrosion resistance. Using nickel base alloy (+') phase strengthening theory, this article select Al and Fe as the third group, and using the method of magnetron sputtering on the Cu/Si substrate to get Cu-Ni-M ternary film. In order to obtain coherent '-Ni3M precipitate phase with matrix, the film composition was designed according to Ni/M ratio of 3. This paper emphatically studied the effect of atomic radius, mixing enthalpy, electronic concentration difference on '-Ni_3M phase morphology, size and distribution. Research results show that Ni/M ratio of Cu-Ni-Al and Cu-Ni-Fe alloy films are 3.1-3.3, 3.8-4.3 respectively according to EPMA composition analysis of sputtering films. After the primeval microstructure and performance characterization for two system part of the film, there have been a portion of '-Ni_3M phase in the Cu-Ni-M sputtering film within the above range of Ni/M ratios, and are embedded in the substrate in nano-state. At this time, the film has a high hardness, which may be caused by the synergistic effect of microcrystalline enhancement caused by nano-columnar crystals and precipitation strengthening caused by '-Ni_3M phase. After annealing at 723 K for 20 h, its hardness can still maintain a high level, which shows good stability of the film.

Keywords: copper alloy film, precipitation strengthening, hardness, heat resistance performance

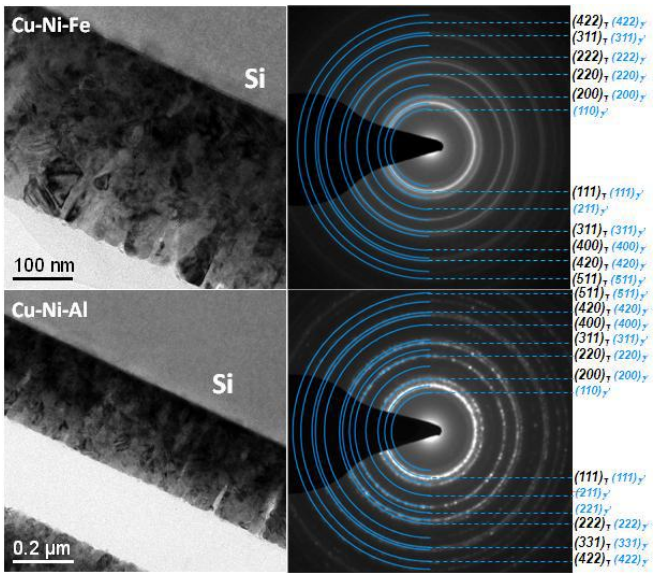

Fig.1

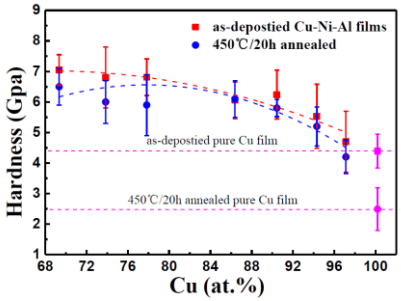

Fig.2

Heterogeneous nuclei effect of $MgAl_2O_4$ in NbC reinforced Fe matrix coating

Changchun Zhao, Xiaolei Xing, Yefei Zhou, Zhijun Shi, Qingxiang Yang
(Yanshan University)
zhaocc0915@outlook.com

Abstract: NbC reinforced Fe matrix composite coatings are widely used for surface strengthening of materials due to their high hardness and high wear resistance. During the solidification process, the order of solidification of NbC and the matrix can make the NbC precipitate in form of granular primary carbides or platy eutectic carbides, and the wear resistance of the granular carbides is more excellent. Some studies have shown that $MgAl_2O_4$ can act as a heterogeneous nucleation center of TiN to promote the precipitation of TiN in acicular ferrite, and found that $MgAl_2O_4$ and TiN have the same crystal orientation with a lattice constant ratio of 2:1. NbC and TiN have the same crystal structure, and the NbC is more compatible in terms of the crystal lattice. However, the bond between them remain to be studied. Therefore, we hope to study the bonding structure between NbC and $MgAl_2O_4$, and then promote the precipitation of NbC in the form of granular primary carbides by $MgAl_2O_4$ to improve the wear resistance of the coating.

In order to study the binding between $MgAl_2O_4$ and NbC, the $MgAl_2O_4$ (111) plane and the NbC (111) plane were overlapped. There are six different element combinations: Mg-Nb, Mg-C, Al-Nb , Al-C, O-Nb and O-C, and previous studies have shown that the surface energy of $MgAl_2O_4$ (111) surface has the following relationship: Mg(O)<Al(Mg)<O(Mg)<O(Al)<O2(Al)<Mg(Al)<O2(Mg)<Al(O). The lower surface energy, the more stable it is, therefore, the most stable Mg(O), Al(Mg) and O(Mg) is selected. During the calculation, the geometrical optimization of O(Mg)C and Mg(O)Nb laps does not converge, so only the four laps of Mg(O)C, Al(Mg)Nb, Al(Mg)C and O(Mg)Nb were discussed. The charge density plot shows that there are electron orientation distributions at the four overlap interfaces, indicating that covalent bonds are generated. From the differential charge density, it can be observed that the electrons at the four interfaces all have electron gain and loss regions, indicating the generation of ionic bonds. The bond populations analysis at the interface reveals that the value of Mg(O)C interface is negative, indicating that an unstable antibond is generated between Mg-C, while the other interface is positive, indicating the formation of covalent bond. It shows that Al(Mg)Nb, Al(Mg)C and O(Mg)Nb have good bonding properties.

The coating with MgAl alloy powder added were prepared. XRD results showed that, the coating is composed of MC carbides, α-phase and γ-phase. The SEM results are shown in Fig. 2, the primary carbides and eutectic carbides can be clearly observed. In addition, the core-shell structure can be observed in some granular primary carbides. The elements of Mg, Al, and O tested by EDS are found to be high in the core, and their atomic ratios were very close to 1:2:4. The core shell structure can also be found in the TEM results shown in Fig.3. In the structure, the core crystal is a face-centered cubic structure with a crystal axis direction of [112] and a lattice constant of 8.17 Å. It is consistent with the crystal structure of $MgAl_2O_4$ and is close to the lattice constant of 8.09 Å measured with $MgAl_2O_4$, which confirms that this core crystal is $MgAl_2O_4$. The core-shell structure is composed of NbC shell and $MgAl_2O_4$ core.

NbC has good lattice matching with MgAl2O4, and the calculated results show that Al(Mg)Nb, Al(Mg)C and O(Mg)Nb interface has a good combination. From the experiment results, $MgAl_2O_4$ can be observed as the core of the core-shell carbides, indicating that MgAl2O4 can be used as a nucleation core to promote the precipitation of NbC carbides.

Keywords: $MgAl_2O_4$, heterogeneous nuclei, bonding structure

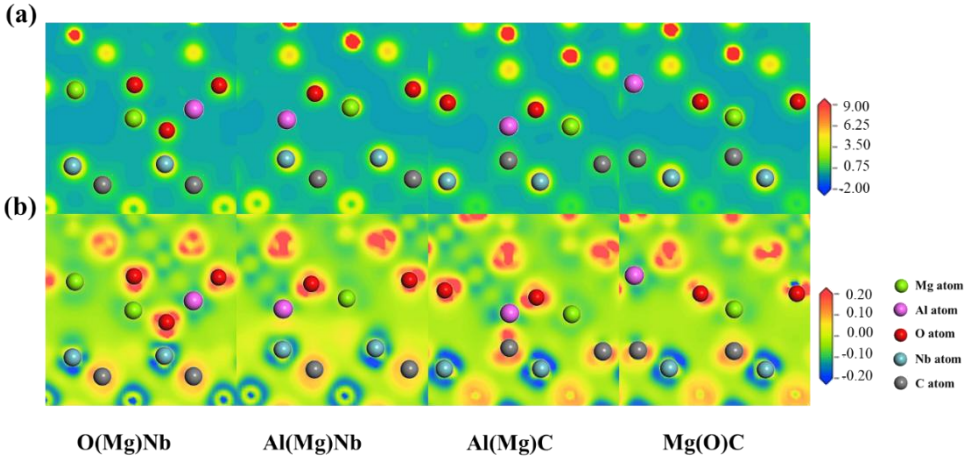

Fig.1

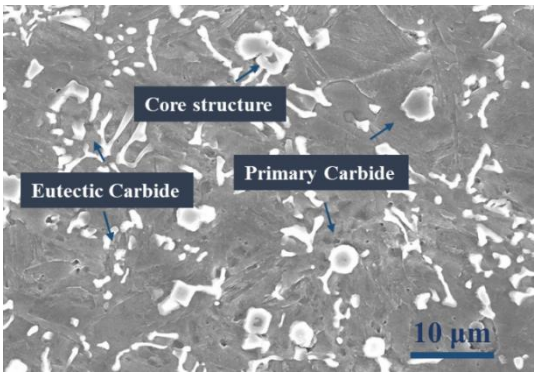

Fig.2

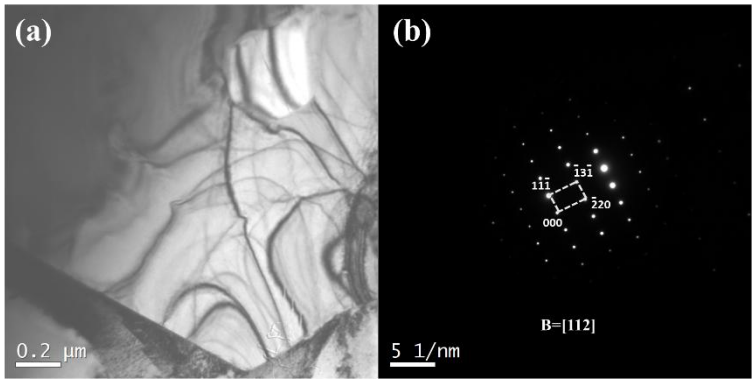

Fig.3

Competitive growth of $Al_2O_3/Y_3Al_5O_{12}/ZrO_2$ in the eutectic ceramic during directional solidification: effect of interface strain energy

Xu Wang[1], Jingyang Wang[2], Langhong Lou[2], Jian Zhang[2]
(1. School of Materials Science and Engineering, Xi'an University of Technology, Xi'an 710048, China;
2. Institute of Metal Research, Chinese Academy of Sciences, Shenyang 110016, China)
xuwang@xaut.edu.cn

Abstract: The microstructure evolution and growth behavior of the $Al_2O_3/Y3Al_5O_{12}/ZrO_2$ ternary eutectic ceramic during directional solidification were well investigated. The most interesting topic of the article was that interface strain energy plays a decisive role in affecting the crystallographic orientation and components (interfaces and phases) distribution in the $Al_2O_3/Y_3Al_5O_{12}/ZrO_2$ eutectic. We found that Al_2O_3 paralleled ZrO_2 while that did not parallel $Y_3Al_5O_{12}$ at the middle of the crystal (~ 50 mm from the seed bar), which might be attributed to the minimum interface strain energy of Al_2O_3/ ZrO_2. Besides, it was observed that the interfaces of Al_2O_3/ZrO_2 and $Y_3Al_5O_{12}/ZrO_2$ are shorter and more dispersed than that of the $Al_2O_3/Y_3Al_5O_{12}$. The area percentage of the Al_2O_3/ZrO_2 and YAG/ZrO_2 interfaces are (40.4±0.2)% and (30.8±0.1)%, respectively, higher than (28.8±0.2)% of the Al_2O_3/YAG. However, the content of Al_2O_3 and $Y_3Al_5O_{12}$ phases are 39.9% and 41.1%, respectively, almost double of that of ZrO_2. These results were discussed based on the coincident site of atoms at as-determined interface, the calculation of the interfaces deregister, together with the considering of the as-satisfied ionic charge balance. It was found that Al_2O_3/YAG interfaces possess higher interface strain energy and thus are not expected during directional solidification. Therefore, tiny ZrO_2 phases were commonly found between the YAG and Al_2O_3, reducing the content of Al_2O_3/YAG interfaces, and leading to short and dispersed interfaces of Al_2O_3/ZrO_2 and YAG/ZrO_2. This study can provide theoretical guidance for selecting of the new toughening phase for binary eutectic ceramics.

Keywords: directional solidification, interface structure, crystallographic orientation, ceramic

Influence of intercritical quenching heat treatment on the mechanical properties of a high nickel steel

Guojin Sun[1], Mingke Li[2], Zhiyuan Zhang[1], Demei Zhai[1], Guang Su[1]
(1. Henan Institute of Technology; 2. Henan Tianli Thermal Equipment Co., Ltd.)
sunguojin@sohu.com

Abstract: This paper investigates the influence of quenching + tempering (QT) treatment and quenching + intercritical quenching + tempering (QLT) treatment on the mechanical properties of a high nickel steel. Compared with rolling condition, the properties of impact toughness and tensile strength are evaluated from the mechanical tests. Results show that after QT and QLT treatment, both tensile strength and impact toughness are increased compared with that under initial rolling condition. Tensile strength will decrease slightly after QLT treatment but the impact toughness will modified greatly compared with that after QT treatment. Metallographic analysis confirms that the modification of mechanical properties after QLT treatment can be attributed to the refinement of grain size and formation of stable austenite. The fractograph of impact specimens under different conditions are also discussed in this paper.

Keywords: QLT treatment, QT treatment, mechanical properties, mechanical properties, microstructure

The influence of centerline segregation on the mechanical performance and microstructure of X70 pipeline steel

Fujian Guo[1], Xuelin Wang[1], Wenle Liu[1], Chengjia Shang[1,2], R. D. K. Misra[3], Hua Wang[4], Tan Zhao[4], Chunlin Peng[4]

(1. Collaborative Innovation Center of Steel Technology, University of Science and Technology Beijing, China
2. State Key Laboratory of Metal Materials for Marine Equipment and Applications, China;
3. Department of Metallurgical and Materials Engineering, University of Texas EI Paso, USA;
4. Technology Center, Anshan Iron and Steel Group Company, China)

Abstract: Centerline segregation is an inherent phenomenon when the solute elements concentrate in mid-thickness of the slab during solidification. It can be controlled by optimizing the continuous casting process, but not easy to be avoided. According to the severity of centerline segregation of the slab, it will affect the mechanical properties and final microstructure of rolled strip. The objective of this paper is to study the influence of centerline segregation degree on the microstructure and mechanical properties of X70 pipeline steels (API 5L grade). The results illustrated that the fraction of segregated region in hot-rolled strip was in accordance with that assessed in continuously cast slab, and the morphology of segregated area in strip presented as discontinuous or continuous band depending on its severity. In this study, the mechanical properties of strips produced from the slabs were examined and the results showed that centerline segregation was some adverse effect on Charpy impact toughness and tensile properties of hot-rolled strips. The strips from slab with higher degree of segregation, exhibited lower Charpy impact toughness, higher tensile strength, higher microhardness. The segregated degree of slab was studied by using the method of Mannesmann, indicating that it could be up to class 3-4. Moreover, the results from Electron Probe Micro Analyzer (EPMA) showed that high level of Mn content was obtained at the centerline of strips processed from the slab with segregation degree of class 3-4. The corresponding microstructure was identified as lath martensite, which should be contributed to the undesirable mechanical properties.

Keywords: centerline segregation, mannesmann rating, microstructure, mechanical performance

Development of EET method and its application

Cheng Lin, Guili Yin, Jianzhong Wang
(School of Materials Science and Engineering, Liaoning University of Technology, China)
cheng_lin1979@163.com

Abstract: The empirical electronic theory (EET) of solids and molecules was proposed by Ruihuang Yu in 1978. So far, EET has been widely used in the field of material science, but its development is still slow. In this paper, the bond length difference (BLD) and its improvement is reported, the solid -state phase transformations in titanium alloys were also reported, the theoretical calculation methods for mechanical properties of alloys were exhibited

Keywords: EET, bond length difference (BLD), development, application

Application of cellular automaton approach in modeling the austenite-to-ferrite transformation in steels

Chengwu Zheng
(Institute of Metal Research, Chinese Academy of Sciences)
cwzheng@imr.ac.cn

Abstract: The austenite-to-ferrite transformation in steels has attracted much attention in view of its close correlation with not only fundamentals of the solid phase transformation theory but also its potential practice relevance with final microstructures and properties of the steel product. With the recent development of microstructure-based mesoscale models, the approach of integrated microstructural simulation is ideally suited to provide deeper insights into the mechanism, transition kinetics as well as the morphology complexity of this phase transformation. Among the various mesoscopic models, the cellular automaton method is a promising tool for predicting and understanding the microstructural phenomena of the austenite-to-ferrite transformation in steels in view of its convenience to include the microstructure related concept and thus become phenomenologically sound to simulate the microstructure evolutions at the grain scale. In the last two decades, an extensive body of CA models was available for the austenite-to-ferrite transformation in steels. Here, the status of the CA modeling regarding the austenite-to-ferrite transformation is going to be briefly reviewed. Special attention is given to the underlying metallurgical concepts implemented in microstructure-based CA modeling of the austenite-to-ferrite transformation.

Keywords: austenite-to-ferrite transformation, cellular automaton, microstructrure evolution, steels, mesoscale modeling

Experimental investigation of massive transformation in ultra-low carbon steel

Hengchang Lu[1], Jianhui Liu[1], Cunyu Wang[1], Li Meng[1], Han Dong[2]
(1. Central Iron & Steel Research Institute; 2. Shanghai University)
282503825@qq.com

Abstract: The characteristics, influence factors and kinetics of massive transformation in ultra-low carbon steel (pure iron, IF steel) were investigated by using thermodilatometry, hot compression test, and heat treatment, respectively. The results show that two kinds of morphology of massive ferrite were obtained for different supercooling degree. When the degree of supercooling is at range of 20-115 ℃, the morphology of massive ferrite is polygonal and named here as Fp. When the supercooling degree is larger than about 200 ℃, the massive ferrite was named as FS with abundant sub-structure. Coarser austenite grain, larger cooling rate, excessive component of niobium and deformation can promote the formation of FS massive ferrite. The strength of steel can be enhanced for increasing the amount of FS massive ferrite by means of sub-structure strengthening. The order of magnitude of interphase velocity for massive ferrite is 10-5m/s. Massive transformation can be induced to occur by hot deformation and the true stress-true strain curve is gradually decreasing correspondingly.

Keywords: massive transformation, ultra-low carbon steels, kinetics, substructure

Effects of Mo/Zr minor-alloying on the phase precipitation behavior in modified 310S austenitic stainless steels at 700 ℃

Donghui Wen[1], Qing Wang[1], Rui Tang[2], Chuang Dong[1]
(1. Dalian University of Technology; 2. Nuclear Power Institute of China)
wangq@dlut.edu.cn

Abstract: High-Cr/Ni austenitic stainless steels (ASSs) have attracted more attention as fuel cladding materials of supercritical water reactors due to their excellent comprehensive properties. In order to further improve their microstructural stability at high temperatures, the present work investigated systematically the influences of Mo/Zr contents and Zr/C ratios on the phase precipitation behaviors and mechanical properties of modified 310S ASSs. The designed alloy ingots were hot-rolled, solid-solutioned at 1423 K for 0.5 h, stabilized at 1173 K for 0.5 h, and then aged at 973 K for different hours. The microstructure and precipitated phases at different heat-treatment states were characterized with OM, SEM, EPMA and TEM, respectively. All the results indicated that the excess addition of Mo and Zr and the inappropriate Zr/C ratios would promote the formation of $Cr_{23}C_6$, G-Ni16Si7Zr6 and (Ni,Fe)23Zr6 phases, resulting in the sigma phase precipitation at the early stabilization stage. Furthermore, the formation mechanism of sigma phase was discussed. The effects of the precipitated phases on the mechanical properties of alloys were then studied. It was found that the Fe-22Ni-25Cr-0.046C-0.37Mo-0.35Zr (wt%) alloy with appropriate Mo content and Zr/C ratio of 1/1 exhibits the best microstructural stability and good tensile mechanical property, in which only a few sigma particles are precipitated from the matrix even after aging at 973 K for 408 h.

Keywords: austenite stainless steels, minor-alloying, microstructural stability, precipitation behavior

Designing of coherent microstructure with cuboidal nanoprecipitates in multi-component alloys

Qing Wang, Chuang Dong
(Dalian University of Technology)
wangq@dlut.edu.cn

Abstract: The microstructure of cuboidal ordered nanoparticles coherently-precipitated into the disordered solid solution matrix is always expected for superalloys, like Ni-based superalloys. However, it is difficult to achieve such kind of morphology in B2 order-strengthened BCC alloys due to an immoderate lattice misfit caused by a larger composition difference between them. The multi-principal component alloying of high-entropy alloys (HEAs) will provide a new composition pathway for adjusting the lattice misfit between BCC and B2. The present work designed a series Al-Ni-Co-Fe-Cr alloys with compositions of [Al-M14]Al in light of the cluster formula approach to investigate the relation between coherent morphologies (weave-like spinodal microstructure, spherical precipitation, and cuboidal precipitation) and lattice misfit of BCC and B2. Among them, the microstructure of cuboidal B2 nanoprecipitation into the BCC matrix renders the HEAs with not only high strength but also good ductility, like those in Ni-base superalloys, i.e., cuboidal L12 nanoparticles embedded in FCC matrix. Then, the optimal strengthening as a function of the shape and size of the coherent precipitates is discussed via the lattice misfit in alloys. The formation rule of cuboidal nanoprecipitation in multi-component alloy systems is also investigated.

Keywords: multi-component alloys, coherent microstructure, particle shape, precipitation strengthening mechanism

Grain boundary-constrained reverse austenite transformation in nanostructured Fe alloy: model and application

Linke Huang[1], Weitong Lin[1], Kang Wang[1], Shaojie Song[1], Can Guo[1], Yuzeng Chen[1], Yujiao Li[2], Feng Liu[1]
(1. State Key Laboratory of Solidification Processing, Northwestern Polytechnical University, Xi'an, China; 2. ZGH, Ruhr-University Bochum, Universitätsstr, 150, 44801 Bochum, Germany)
hfuthlk@163.com

Abstract: reverse austenite transformation (RAT) is critical for designing advanced high-strength steels (AHSS), which, however, has not been sufficiently studied in nanostructured (NS) steels or Fe alloys, and hence not fully understood yet. Herein, the RAT (e.g. ferrite to austenite) kinetics in the NS Fe alloy upon continuous heating was experimentally and theoretically investigated, where, the ultrafine austenite characterized by a sluggish growth velocity and a high thermal stability, and additionally, an appreciable solute partitioning detected using atom probe microscopy, indicate the diffusion-controlled mechanism of RAT. The double-edged role of grain boundaries (GBs) in the NS alloy is elucidated, i.e. enhancing the diffusivity due to the type-A kinetics, and simultaneously, facilitating the formation of constrained diffusion field mainly due to the segmented effect of GB nucleation. On this basis, a modified diffusion model incorporating the effect of GBs is implemented to understand the GB-constrained austenite growth and the associated partitioning behavior, and further complemented with Cahn model, an austenite growth model is applied to predict the overall kinetics of RAT in the NS Fe alloy. It then follows that a strategy by combination of diffusion-controlled growth model and microstructure model could serve as a framework to predict the kinetics of RAT in the NS alloys. Regarding the RAT kinetics in the NS alloys, the present work uncovers the 'GB-constrained' mechanism, which is expected to offer the potential application for nanostructure manipulation in the development of AHSS.

Keywords: phase transformation, nanostructured metals, thermo dynamics, kinetics

On composition and growth mechanism of LPSO structure in an Mg-Zn-Gd alloy

Xinfu Gu
(University of Science and Technology Beijing)
xinfugu@ustb.edu.cn

Abstract: Long period stacking ordered (LPSO) structures in Mg-TM-RE alloy (TM: transition metal, RE: rare earth element) contribute to improved mechanical properties at both room temperature and elevated temperature. The LPSO structure often consists of regular arrangements of solute-enriched FCC structural units (SU). The stacking order of SU can be changed from HCP by a <1-100>/3 type partial dislocation. Since the transformation strain is significant, the accommodation of the transformation strain at the growth ledge should be considered. Based on the elastic interaction energy between neighbor SUs, we have proposed the possible low energy configuration, i.e. the transformation strain should be self-accommodated. However, the actual dislocation configuration for growth ledge consisting of multiple SUs is unknown. In this study, we aim to clarify the possible dislocation configuration by using three-dimensional atom probe (3DAP) and Cs-corrected high-angle annular dark field (HAADF) STEM.

Keywords: magnesium, strain accommodation, interaction energy, HAADF-STEM

Correlation between electrical resistivity and microhardness of Cu alloys via a short-range-order cluster model

Chuang Dong
(Key Laboratory of Materials Modification, Dalian University of Technology)
dong@dlut.edu.cn

Abstract: For Cu alloys, both strength and electrical resistivity are required in practice, but the two properties are contradictory to each other. The present work analyzes the dependence of hardness and electrical resistivity on solute contents for ternary $[Mo_{y/(y+12)}Ni_{12/(y+12)}]_xCu_{100-x}$ alloys (at%), with x=0.3-15.0 being the total solute content and y=0.5-6.0 the ratio between Mo and Ni. The alloys are designed following the cluster-plus-glue-atom model to reach three distinct structural states, i.e., cluster solution state (y=1), where Mo is dissolved via a chemical short-range-order characterized by Mo-centered and Ni-nearest-neighbored [Mo1-Ni12] cluster, cluster solution state plus extra Ni solution (y<1), and a cluster solution state plus extra Mo in precipitation (y>1). The measured electrical resistivity and microhardness data are correlated to these three structural states to reveal the property dependences on solute contents. The cluster solution enhances the strength, without causing much increase in the electrical resistivity, as the solutes are organized into cluster-type local atomic aggregates that decrease dislocation mobility more strongly than electron scattering. In analogy to residual resistivity R, which indicates the change of resistivity with reference to pure Cu, residual microhardness HR and residual lattice constant aR are also defined. For the ideal cluster solution state (y=1, Mo/Ni=1/12), the above three parameters are correlated to the total solute content x by R=1.08 x (10^{-8} Ω·m), HR=1.50 x (kgf mm^{-2}), and aR=–1.08 x (10^{-4} nm). From these, R=0.72HR=–aR. Such simple relationships indicate that resistivity and strength are dependent on the same cluster-type solution mechanism and can be a good reference for evaluating strength and resistivity performance of Cu alloys.

Keywords: electrical resistivity, cluster-plus-glue-atom model

Chemical short-range orders and the induced structural transition in high-entropy alloys

Yue Ma, Qing Wang, Chuang Dong
(Dalian University of Technology)
wangq@dlut.edu.cn

Abstract: The chemical short-range orders (CSROs) of high entropy alloys (HEAs) play an important role in their structural transitions and advanced properties. However, it is difficult to describe the CSROs with local atomic structures. The present work introduces a cluster-plusglue-atom model to understand the CSROs of Al-Ni-Co-Fe-Cr HEAs, which dissociates the solid-solution structure into a cluster part and a glue atom part. Two HEAs with a composition of Al2M14 (M presents different combinations of transition metals) are designed, which are derived from two cluster models of [Al-M12](M2Al1) in the FCC structure and [Al-M14]Al1 in the BCC structure. M=Ni4Co4Fe3Cr3 renders the HEA with a FCC-based structure, while the matrix will transform into a BCC structure when M=Ni1Co1Fe2Cr1. These two cluster models are then used to simulate the pair distribution function (PDF) at short inter-atomic distances. The calculated PDFs within the frame of the cluster models can describe the neutron PDFs better than the ones based on average crystal structures. It provides a clear indication of the existence of CSROs in HEAs and proves the feasibility of the cluster structural model. This model demonstrates a novel way to understand the CSROs and the induced structural transition due to the local lattice distortion, which would be developed into a new alloy design strategy for high-performance HEAs.

Keywords: high-entropy alloys, chemical short-range order, cluster structural model, neutron scattering

Multi-stage martensitic transformation behaviors and microstructural characteristics of Ti-Ni-Hf high temperature shape memory alloy powders

Xiaoyang Yi, Xianglong Meng, Zhiyong Gao, Wei Cai
(Harbin Institute of Technology)
xlmeng@hit.edu.cn

Abstract: The as-received Ti-49Ni-15Hf (at%) alloy powders fabricated by the plasma rotating electrode process (PREP) exhibited the abnormal multi-stage martensitic transformations, which were largely dependent on the particle size. Upon heating and cooling process, the Ti-Ni-Hf alloy powders with the size of 0-75 μm and 75-150 μm showed the two-stage and the three-stage martensitic transformation, respectively. The multi-stage transformations were all corresponding to the B2B19′ martensitic transformation. During the rapid solidification, the existence of the distinctive cooling rate as well as the presence of $(Ti,Hf)_2Ni$ precipitates resulted in the inhomogeneous spatial distribution of Hf concentration, which is the main reasons for the appearance of the multiple stages martensitic transformation.

Keywords: Ti-Ni-Hf alloy powder, shape memory alloy, rapid solidification, multi-stage martensitic transformation, microstructure

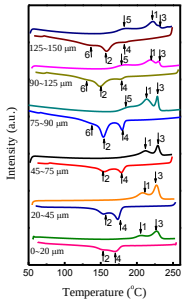

Fig.1

Microstructure and property characterization of Al0.4CoCu0.6NiSi0.2 high entropy alloy powder for additive remanufacturing prepared by gas atomization

Yongxing Chen[1], Sheng Zhu[1], Xiaoming Wang[1], Liu Qiu[1], Guofeng Han[1], Shu Wen[2]
(1. National Key Laboratory for Remanufacturing, Army Academy of Armored Forces;
2. School of Materials Science and Engineering, Xiangtan University)
zusg@sohu.com

Abstract: The work prepared Al0.4CoCu0.6NiSi0.2 high entropy alloy powder by gas atomization method and analyzed the powder's particle size distribution, phase composition, microstructure, thermal stability, surface chemical elements state, microhardness and elastic modulus using particle size analyzer, X-ray Diffraction (XRD), Optical Microscope (OM), scanning electron microscope (SEM), different scanning calorimetry (DSC), X-ray photoelectron spectroscopy (XPS), hardness tester and nano-indenter. The results showed that most of the prepared powder was in the particle size range of 50-150 μm (about 80%), which was suitable for the coaxial feed powder of additive remanufacturing, and the powder's phase structure was consisted of fcc + minor bcc solid solution. The highest hardness value of the powder reached 392 HV. The elastic modulus was about 200 GPa. The strength and plasticity of the powder was excellent overall, and it can be used for 3D printing or additive remanufacturing.

Keywords: gas atomization, high entropy alloy powder, microstructure, mechanical property, additive remanufacturing

Enhanced strength and ductility of A356 cast aluminum due to composite effect of non-equilibrium solidification and thermomechanical treatment

Xu Zhang, Linke Huang, Yuzeng Chen, Feng Liu
(State Key Laboratory of Solidification Processing, Northwestern Poly-technical University)
liufeng@nwpu.edu.cn

Abstract: Compared to wrought Al alloy, conventional Al-Si casting alloy always show poor tensile strength and less ductility, which is difficult to enhance mechanical performance through deformation at room temperature. Here, we designed a special route by combining sub-rapid solidification with four passes of ECAP and intermediate heat treatment to refine and homogenize cast microstructure. After the first step treatment, elongation to failure of the alloy was as high as 29%, which provided the ability for further composite severe plastic deformation (ECAP+rolling) with pre-deformation aging treatment of step II. The evolution of microstructure and mechanical properties at various stages were systematically investigated. After processed by this integrated treatment, the ultimate tensile strength and elongation to failure of A356 alloy were 517 MPa, 7%, respectively. The optimization of the morphology of eutectic silicon particles of step Ⅰ is the main factor to further improve the ductility of A356 alloy. Dislocation strengthening and precipitation strengthening play a more significant role in improving the strength of A356 alloy of step II. In addition to superior castability, Al-Si based casting alloy also has good welding and high wear resistance that superior to some wrought Al alloy, therefore, our research is expected to expand the use range of Al-Si casting alloy and replace wrought Al alloys in some fields.

Keywords:A356 alloy, sub-rapid solidification, two steps of TMT, strength, ductility.

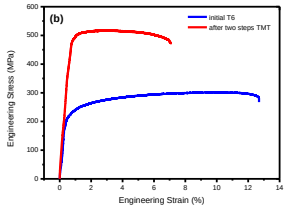

Fig.1

Cubic martensite in high carbon steel

Yulin Chen, Xinqing Zhao
(School of Materials Science and Engineering, Beihang University)
xinqing@buaa.edu.cn

Abstract: A distinguished structural characteristic of martensite in Fe-C steels is its tetragonality originating from carbon atoms occupying only one set of the three available octahedral interstitial sites in the body-centered-cubic (bcc) Fe lattice. Such a body-centered-tetragonal (bct) structure is believed to be thermodynamically stable because of elastic interactions between the interstitial carbon atoms. For such a phase stability, however, there has been a lack of direct experimental evidence despite extensive studies of phase transformations in steels over one century. In this letter, we report that the martensite formed in a high carbon Fe-8Ni-1.26C (wt%) steel at room temperature induced by applied stress/strain has a bcc rather than a bct crystal structure. This finding not only challenges the existing theories on the stability of bcc vs. bct martensite in high carbon steels, but also provides new insights into the mechanism for martensitic transformation in ferrous alloys.

Keywords: high carbon steel, microstructure, body-centered-cubic, phase transformation

Cluster formulas of Co-Al-W-base superalloys

Qihui Ma, Chuang Dong
(Key Laboratory of Materials Modification by Laser, Ion and Electron Beams Ministry of Education, Dalian University of Technology)
dong@dlut.edu.cn

Abstract: Having a similar two phases γ/γ′ microstructure to Ni-base superalloys and also including various alloying elements such as Al and W, new Co-base superalloys—Co-Al-W-base alloys have been widely studied as a kind of potential alternatives of Ni-base superalloys, which are the most important high temperature structural materials in industrial applications. Besides, Co-Al-W-base alloys also have excellent mechanical properties, for example, creep properties comparable to those of the first generation Ni-base single crystal superalloys. However, in the Co-Al-W ternary phase γ/γ′ two phases region is too narrow, γ′ phase has poor thermal stability and alloys have low high temperature strength. Alloying is necessary for design of alloy composition to expand two phases region and improve solvus temperature of γ′ phase. And finding an effective alloy composition method can greatly improve efficiency. A cluster-plus-glue-atom structure model which can be applied to design complicated multi-element alloy composition has been put forward in long-term research of composition rules of amorphous alloys and quasicrystals. In our previous work, ideal composition formula of Ni-base superalloys has been obtained by applying the cluster-plus-glue-atom structure model of faced centered cubic solid solutions, which finds that the most stable chemical short-range-order unit is composed of a nearest-neighbor cluster and three next-neighbor glue atoms. In this paper, the ideal cluster formula of CoAl-W-base superalloys is addressed using the same approach. Based on cluster-plus-glueatom model theory, according to lattice constants by experiments and atom radii, calculations are carried out. Results show that the atom radius of Al is equal to Covalent radius-0.126 nm in both γ and γ′ phases because of the strong interaction between Co and Al, and for γ′ phase the atom radius of W changes obviously, reducing to 0.1316 nm. After calculating atomic radii, the basic chemical formula for Co-Al-W ternary alloys is calculated, [Al-Co_{12}](Co, Al, W)$_3$, signifying an Al centered atom and twelve Co nearest neighbored cluster atoms plus three glue atoms which is in good agreement with Ni-base single crystal superalloys. For multi-element alloys, firstly the alloying elements are classified, according to the heats of mixing between the alloying elements and Co, into solvent elements-Co like elements (Co, Ni, Ir, Ru, Cr, Fe, Re) and solute elements -Al like elements. The latter is further grouped into Al, W (W and Mo, having weaker heat of mixing than Al-Co) and Ta(Ta, Ti, Nb, V, etc, having stronger heat of mixing than Al-Co). Then all chemically complex Co-Al-W-base superalloys are simplified into Co-Al pseudo-binary or Co-Al-(W, Ta) pseudo-ternary systems. After screening, alloy compositions have been analyzed and alloying elements are placed into basic formula-[Al-Co_{12}](Co, Al, W)$_3$. Within the framework of the cluster-plus-glue-atom formulism and analyzing composition rule, CoAl-W-base superalloys satisfy the ideal formula. [Al-Co_{12}]($Co_{1.0}Al_{2.0}$)=[AlCo_{12}]$Co_{1.0}Al_{0.5}$(W, Ta)$_{1.5}$=$Co_{81.250}Al_{9.375}$(W, Ta)$_{9.375}$. By the same way, those of γ and γ′ phases are respectively [Al-Co_{12}]($Co_{1.5}Al_{1.5}$)=[Al-Co_{12}]$Co_{1.5}Al_{0.5}$(W, Ta)$_{1.0}$=$Co_{84.375}Al_{9.375}$(W, Ta)$_{6.250}$ and [Al-Co_{12}]($Co_{0.5}Al_{2.5}$)=[AlCo_{12}]$Co_{0.5}Al_{0.5}$(W, Ta)$_{2.0}$=$Co_{78.125}Al_{9.375}$(W, Ta)$_{12.500}$. And the alloy formula can be regarded as the equal proportions of phase formulas. For example, alloy Co82Al9W9 and its γ and γ′ phases are formulated respectively as [Al-Co_{12}]$Co_{1.1}Al_{0.4}W_{1.4}$≈[AlCo_{12}]$Co_{1.0}Al_{0.5}W_{1.5}$, [Al-Co_{12}]$Co_{1.6}Al_{0.4}W_{1.0}$≈[Al-Co_{12}]$Co_{1.5}Al_{0.5}W_{1.0}$, and [AlCo_{12}]$Co_{0.3}Al_{0.5}W_{2.2}$≈[Al-Co_{12}]$Co_{0.5}Al_{0.5}W_{2.0}$.

Keywords: Co-Al-W-base superalloys, composition formula, cluster-plus-glue-atom model, chemical short-range order

Study on the thermal stability of nanoscale bainite/martensite steel

Xinpan Yu, Huibin Wu, Fanfan Feng, Lixiong Xu, Yang Gu, Xintian Wang
(Collaborative Innovation Center of Steel Technology, University of Science and Technology Beijing)
980526406@qq.com

Abstract: The film-like retained austenite in the nanobainitic steel would decompose when it was heated at low temperature, then the bainitic ferrite coarsened and recovery, which bring down the mechanical property of the nanobainitic steel. This paper aims to study on the effect of the prior martensite on the thermal stability of the nanobainitic steel. The nanobainitic steel, consisting of prior martensite, nano-size bainitic ferrite and retained austenite, was obtained by forming partial martensite followed by the bainite transformation at low temperature. The tested was austenitized at 950 ℃, and quenched to 178 ℃ (below Ms about 8 ℃), and then heated preservation at 300 ℃ to accomplish the bainite transformation. The tested samples of the nanobainitic steel were tempered at 200 ℃ and 650 ℃ for 1 h, respectively. Scanning electron microscopy (SEM), X-ray diffraction analyses (XRD) and transmission electron microscopy (TEM) and etc. were utilized to observe the microstructure and the hardness change of the nanobainite steel at different tempering temperatures. The hardness of the tested sample was tested about 10 times to reduce the system error. The results of the experiments showed that the hardness of the nanobainite steel remained at a high level (>500 HV) when the tempering temperature was between 200-500 ℃, and decreased rapidly when the tempering temperature was over 500 ℃, e.g. to 263 HV at 650 ℃. The results of the XRD showed that the retained austenite decomposed between because of the volume fraction of the retained austenite decreased rapidly from 26.5% to 7.2% between 450 ℃ and 500 ℃. The SEM results showed that there are two type of the retained austenite, e.g. blocky retained austenite and film-like retained austenite. The microstructure of the tested nanobainitic steel did not changed at low tempering temperature, especially the prior marstenite. The bainitic ferrite recoveried and formed small ferrite grains at 650 ℃. The lamella bainite contained very fine laths and retained austenite can only be observed through TEM examination due to their small size. From the results of the TEM, we found the thickness of the bainic ferrite remained narrow at 200-350 ℃ (about 60 nm), and then slight coarsened at 350-450 ℃, expanded to 115nm finally at 550 ℃. The bainitic ferrite recoveried and formed small ferrite grains at 650 ℃. Different from the nanobainitic steel from the direct isothermal transformation, the content of the retained austenite in the tested nanobainitic steel exceeded 1.31% which is in the untempered sample, therefore the film-like retained austenite kept stable at the tempering temperature below 450 ℃. According to all the above results and analysis, we thought that decomposition of the film-like retained austenite into carbides at the temperature between 450 ℃ and 500 ℃ resulted in the decrease of the volume fraction of the retained austenite and obviously coarsening of the bainitic ferrite lath during tempering. The prior martensite could keep the carbon content of the retained austenite at a relatively high level when tempering at high temperature (<500 ℃), and delay the decomposition of the retained austenite, and thus improve the thermal stability of the nanobainitic steel.

Keywords: nanobainitic steel, thermal stability, prior marstensite, hardness

Relationship between the crystallographic characteristics and toughness of the prior austenite grains refined by multi-step

Binbin Wu, Chengjia Shang
(University of Science and Technology, Beijing)
cjshang@ustb.edu.cn

Abstract: A low carbon and low alloy system with B design is adopted to develop high strength, high toughness and low alloy steel with thick plates suitable for offshore engineering or large machinery. To produce high strength low alloy (HSLA) steel, the process of quenching and tempering (QT) is required. However, the bainite or ferrite phase transformation occurs because the core of thick plate cannot achieve high enough cooling speed. Adding trace B and refining primary austenite grains can improve the hardenability of steel, to realize martensite phase transformation at low cooling rate and improve the uniformity of the structure and performance of thick plate.

The results showed that the addition of trace B (14 ppm) to steel effectively improved the hardenability of steel, and the refinement of the original austenite grain by multi-step quenching, which further improved the hardenability of steel. The results of SEM indicated that the main microstructure was martensite and lower bainite. Electron Backscattered Diffraction (EBSD) was used to characterize the crystallographic characteristics of once quenching and third quenching of steel, and it was found that the once quenching sample had larger prior austenite grains, belonging to transformation dominated by the Bain grouping. After third quenching, the prior austenite grain is smaller and more uniform, which belongs to the transformation dominated by CP (close-packed plane) grouping. The explanation for this phenomenon is that the increase of the transformation driving force will lead to the transformation change model dominated by the Bain group into the model dominated by the CP group. Using thermal expansion technique to measure Ms points of once quenching and third quenching specimen, the results showed that the Ms of third quenching and once quenching is 423 ℃ and 400 ℃ respectively, indicating that phase transformation driving force increases by multiple quenching. This is because the refined austenite grain increases the non-equilibrium segregation of B at the grain boundary and increases the phase change driving force.

After third quenching, the prior austenite microstructure was refined and homogenized, and the selection of the variant was weakened. As the different Bain groups met to form a large angle grain boundary, more than high angle grain boundaries were formed after three steps of quenching. Mechanical properties testing results show that after third quenching, the –40 ℃ charpy impact energy increased from 33 J to 60 J, consistent with the results of the EBSD.

Keywords: quenching, toughness, hardenability, EBSD, crystallographic characteristics

Influence of quenching and partitioning in bainite zone process on the microstructure and mechanical properties of QP980 steel

Hongying Lü, Xudong Zhou, Xuewen Chen
(Henan University of Science and Technology)
syuuzhou@163.com.

Abstract: To achieve better vehicle weight, QP980 steel as the third generation of advanced high-strength steel began to be used in automotive body stamping parts, however there have been few reports on its heat treatment processes so far. Therefore, in this paper, the quenching-partitioning in bainite zone (Q&PB) heat treatment process was studied on the Gleeble-1500D thermal simulator, as well as the quenching-partitioning (Q&P) process was also carried out as comparative research.

Based on our previous test results that QP980 steel has critical phase transformation point Ac_1=740 ℃, Ac_3=935 ℃, Ms=389 ℃, Mf=258 ℃, we established the Q&PB heat treatment process as follows: specimens were heated at 20 ℃/s to 1000 ℃ for 300 s to complete austenitization, and quenched at 50 ℃/s to different temperatures (330, 350, 370 ℃) for 10 s to obtain a certain amount of martensite and retained austenite, next reheated at 20 ℃/s to 420 ℃ and held for 260 s to make carbon diffuse from martensite to austenite, and finally quenched to room temperature on the Gleeble-1500D thermal simulator; specimens were heated to 1000 ℃ for 300 s, then quenched to 350 ℃ for 10 s, next reheated to different partitioning temperatures (440, 460 ℃) for 260 s, and finally also cooled to room temperature on the same simulator. The Q&P heat treatment process as follows: specimens were heated to 1000℃ for 300s, then quenched to 324 ℃ for 10s, next reheated to different temperatures (360 ℃, 390 ℃, 420 ℃) for 260 s, finally cooled to room temperature. The mechanical properties of the specimen after heat treatment were tested by Gleeble1500D thermal simulator too and the best result is tensile strength of 1543.35 MPa, elongation of 18.7%, and product of strength and ductility of 28.86 GPa % at quenching temperature of 350 ℃ and partitioning temperature of 420 ℃ in the Q&PB process. The corresponding microstructure of the sample is lath martensite, bainite and retained austenite observed by optical microscopes Zeiss Axio Vert A1 and scanning electron microscopes JSMIT100. While the other best result is tensile strength of 1588 MPa, elongation of 17.4%, and product of strength and ductility of 27.64 GPa % at quenching temperature of 324 ℃ and partitioning temperature of 390 ℃ in the Q&P process, and the corresponding microstructure of the sample is lath martensite and retained austenite.

The Q&PB process has some improved both the product of strength and ductility of QP980 steel. This is because there are more carbon-rich retained austenite left to room temperature and carbide-free bainite formed, which is caused by the inhibited of carbides precipitation in bainite by Si.

In the actual use, if you pay attention to the higher strength, then the Q&P process would be chosen; if you are interested in the longer elongation and more product of strength and ductility, then the Q&PB process would be chosen.

Keywords: quenching and partitioning, quenching and partitioning in bainite, zone, multiphase steel, retained austenite, product of strength and ductility

Effects of size on mechanical behavior of Cu40Zr44Al8Ag8 bulk metallic glass

Haorui Liu, Nana Yang, Lei Zhao, Laidong Yang
(School of Mechanical Engineering, Longdong University)
135098281@qq.com

Abstract: Bulk metallic glasses (BMGs) have been widely studied because of their superior mechanical properties, such as high strength and hardness, large elastic limit, superior wear and corrosion resistance. So there is a continuing interest in the mechanical characterization of BMGs. While making large size BMGs, the amorphous structure change with appearing nanocrystalline which influence the strength and plasticity of amorphous metals. In this paper, the relationship of mechanical parameters and size is studied, and the underlying mechanisms of these effects and related fracture behavior were discussed.

The Cu40Zr44Al8Ag8 BMG was chosen for this study. The master alloy was prepared by arc melting a mixture of Zr (99.8%), Cu(99.9%), Al (99.99%), and Ag (99.9%) in a high-purity argon atmosphere, then the melted alloy was suction cast into three different size in water-cooled Cu mold.

The amorphous structure of the samples was confirmed with D/max-2400 X-Ray diffraction (XRD) using Co-Kα radiation. Compression tests were conducted using an Instron 4466 testing machine at an initial strain rate of 1×10^{-4} s^{-1} at room temperature. Following the compression tests, all the specimens were examined by by a JSM-6700F scanning electron microscope (SEM).

The compressive deformation and fracture features of Cu40Zr44Al8Ag8 bulk metallic glassy samples with different dimensions i.e. 2, 4, 6 mm in diameter have been investigated. As shown in Fig.1, The XRD results shows that the crystalline volume fraction is higher when the size increase. The 2mm-diameter sample has typical patterns of amorphous structures with only a broad diffraction halo, and no peaks of crystalline phases can be seen. When the size is increased to 4mm and 6mm, peaks of crystallized phases are detected. From compressive stress–strain curves, as shown in Fig.2, both the fracture strength and compressive plastic strain at failure decreases with increasing sample size. SEM observations reveal that the fracture surfaces are different with the changes in size. The compressive fracture surface of 2 mm-diameter sample mainly consists of a vein-like structure, however, the fracture surfaces can be approximately divided into two regions, the shear area and rough area. The shear area has typical vein-like character, and the rough area appears fishbone-shaped veins and radial veins suggesting a typical cleavage fracture during fragmentation. Even some fracture sites of 6 mm-diameter sample are smooth without veins and traces of local melting.

The evidence indicates that Cu40Zr44Al8Ag8 BMG undergoes a transition from apparent plasticity to brittleness when the sample dimensions approach a critical value. The decrease in strength is mainly attributed to influence of the sample size on the plastic fracture mechanism which lead to differences in crystallinity. Also there is an additional influence of the sample size on the higher probability of having more flaws in big samples.

Keywords: bulk metallic glasses, fracture strength, compressive stress-strain

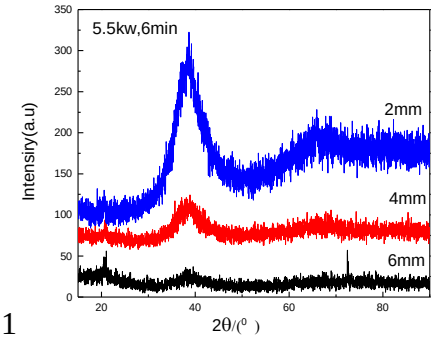

Fig.1

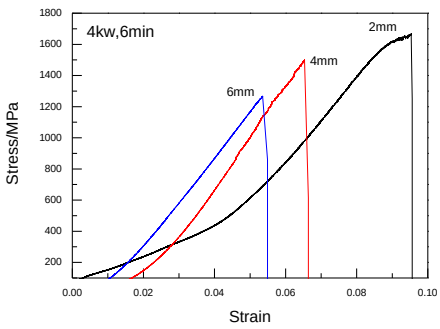

Fig.2

Fig.1 XRD patterns of Cu40Zr44Al8Ag8 metallic glass with different specimen sizes

Fig.2 Compressive engineering strain-stress curves with different specimen sizes at room temperature

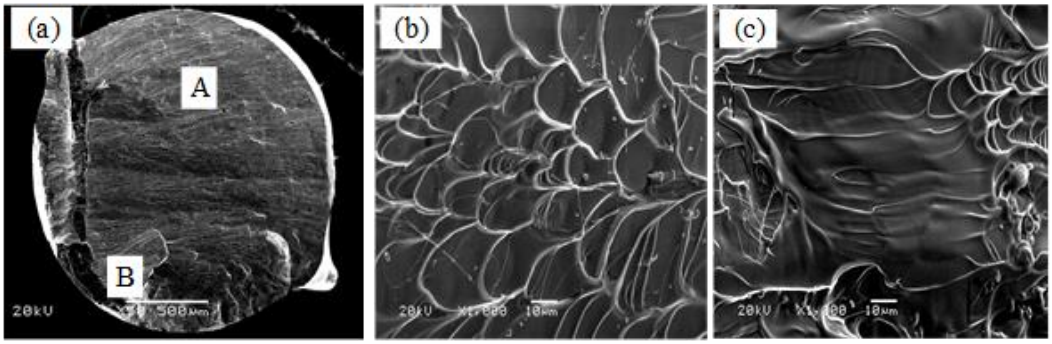

Fig.3 SEM micrographs of fracture surface of 2 mm specimen: (a) low high magnification view of fracture surface; (b) high magnification view of area A; (c) high magnification view of area B

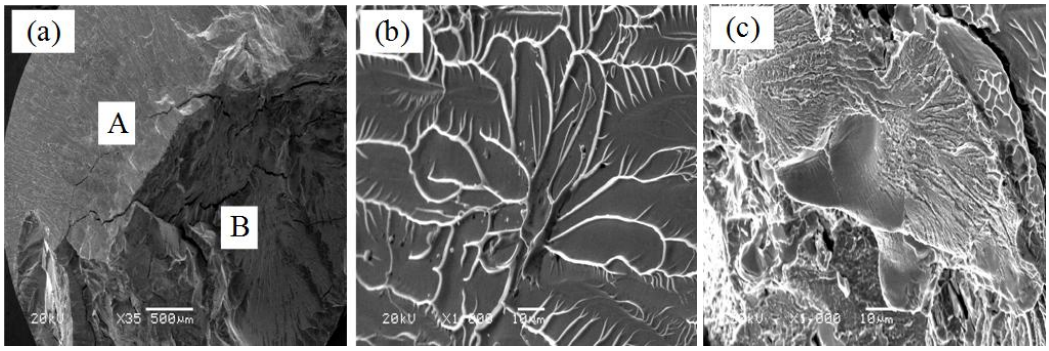

Fig.4 SEM micrographs of fracture surface of 4 mm specimen: (a) low high magnification view of fracture surface; (b) high magnification view of area A; (c) high magnification view of area B

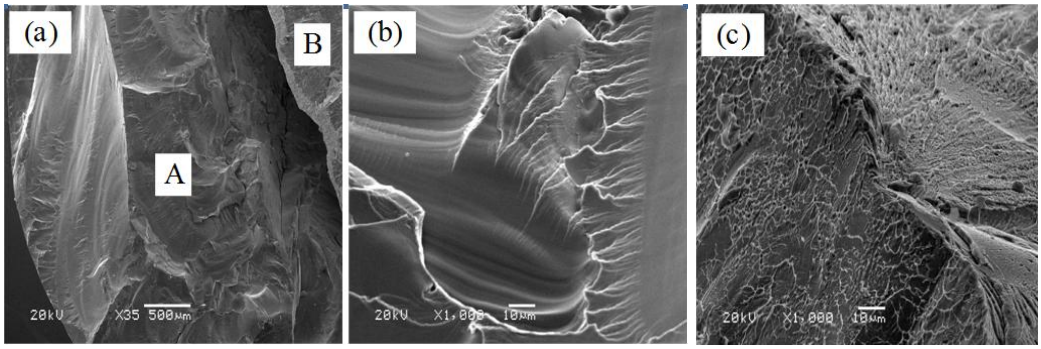

Fig.5 SEM micrographs of fracture surface of 6 mm specimen: (a) low high magnification view of fracture surface; (b) high magnification view of area A; (c) high magnification view of area B

Boriding treatment in quenching-partitioning tempering high strength steels alloyed with niobium and molybdenum

Pedro Gabriel Bonella de Oliveira[1], Fabio Edson Mariani[1], Amadeu N. Lombardi[2], George E. Totten[3], Luiz C. Casteletti[1]
(1. São Carlos Engineering School–University of São Paulo;
2. Federal Technological University of Parana; 3. Portland State University)
pgbonella@gmail.com

Abstract: The heat treatment of quenching and partition (Q&P) has been developed in recent years as a processing alternative for advanced high strength steels (AHSS). In this process, martensite and carbon enriched retained austenite are obtained, allowing excellent combination of resistance and ductility. Due to these properties, steels treated by this technique are potential candidates to the third generation of AHSS, which aims at reducing component weight to promote energy savings and resources, especially in the automotive industry. The treatment consists of quenching to a temperature QT between the start (Ms) and end of martensitic transformation (Mf) temperatures. Then there is the partition step where the material is isothermally held at temperatures above or equal to QT, with the purpose of diffusing carbon from supersaturated martensite into untransformed austenite. The presence of cementite is suppressed by addition of silicon and / or aluminum, thus releasing carbon for austenite enrichment and allowing the effect of transformation induced plasticity (TRIP). The quenching, partitioning and tempering (Q-P-T) process introduces a tempering step to the Q&P treatment, to take advantage of the precipitation hardening effect promoted by carbide forming elements such as niobium and molybdenum. To compensate for the effect of carbide formation during tempering, carbon content in QPT steels is higher than in Q&P steels. Recently, wear performance of advanced steels has been investigated because of their high potential for industrial application. Increased wear resistance is paramount for increase component life and lower maintenance costs. Therefore, the purpose of this work is to incorporate the boriding thermo-chemical treatment to the Q-P-T process, with the purpose of increasing hardness and resistance against surface wear. The characteristics of this treatment makes it a promising alternative for application in these steels since it produces layers of iron borides with high hardness on the material surface. The process is simple, inexpensive and consists of heating the material in a molten salt bath (Borax) above the austenitizing temperature of the steel during 1 to 8 hours. After this period, it is possible to apply all the steps regarding the Q-P-T treatment. In this work samples of steels with 3 chemical composition, with additions of niobium and molybdenum were submitted to boriding treatment followed by Q-P-T. The samples were borided at 900 ℃ for 2 and 4 hours, with direct cooling from that temperature in salt baths at the QT temperature, below Ms. Thereafter, the steels were isothermally held at the partition temperature (PT), above Ms, for 45 minutes and oil cooled. Finally, the tempering step was carried out with heating at 400 ℃ for 2 hours, followed by air cooling to room temperature. The substrate and the layers produced were characterized by optical microscopy (OM), X-ray diffraction (XRD), Vickers microhardness and microadhesive wear tests. The tribological characteristics of the layers were compared with those of the substrate. The results show that the boriding and Q-P-T treatments are feasible, promoting the formation of boride layers on the surface of the steel with mixed microstructure of martensite, bainite and fractions of retained austenite. A great increase in surface wear resistance was observed when compared to the substrate.

Keywords: martensite, retained austenite, boriding, wear resistance

Boro-austempering treatment of high strength bainitic steel alloyed with niobium

Pedro Gabriel Bonella de Oliveira[1], Fabio Edson Mariani[1], Amadeu N. Lombardi[2], George E. Totten[3], Luiz C. Casteletti[1]
(1. São Carlos Engineering School–University of São Paulo;
2. Federal Technological University of Parana; 3. Portland State University)
pgbonella@gmail.com

Abstract: High strength bainitic steels are considered potential candidates for the 3rd generation of advanced high strength steels (AHSS). Leveraged mainly by the automotive industry, the development of this class of alloys seeks to improve safety and reduce vehicle weight, leading to lower fuel consumption. The main characteristic of these steels is the presence of carbide-free bainite. The heat treatment to obtain this microstructure is the austempering. Therein, the material is heated to austenitization, salt bath cooled, isothermally held at temperatures above the martensitic transformation start (Ms) temperature, and then cooled to room temperature. Cementite is a very fragile phase, and usually is a problem when precipitates between the bainitic ferrite plates. Silicon alloying is critical in that regard, suppressing the cementite formation. In consequence, the rejected carbon of bainitic ferrite plates enrich austenite, which becomes metastable at room temperature, promoting the transformation-induced plasticity (TRIP) effect. Other elements added are manganese and molybdenum, for increased temperability and reduction of fragility by impurities, respectively. Niobium alloying has been explored, since it refines the austenitic grain, promoting the increase of bainitic transformation rate. Usually, steels with microstructure fully composed by carbide-free bainite present carbon content close to 1% in weight, deteriorating the weldability. In that way, recent research aims to keep the carbon content below 0, 5%. Due to its high combination of strength and toughness, TRIP steels have been widely used in the transportation, naval and mining industries, making surface wear resistance of great importance, increasing component life and decreasing downtime caused by maintenance work. Boriding is an effective method for increasing wear resistance and also provides high corrosion resistance. The treatment consists in production of layers of iron borides (FeB and Fe_2B), with thickness between 40 and 270 μm and hardnesses that can reach values higher than 2000 HV. Salt bath Boriding is performed at temperatures between 800 and 1100 ℃, with 1 to 8 hours duration, making possible the incorporation of austempering treatment right after the boriding treatment without the need to reheat the parts. The combination of these two treatments is called boro-austempering and is a promising alternative for increasing the wear resistance of AHSS. In the present work, samples of bainitic steels with 3 different chemical compositions, with additions of niobium and molybdenum were submitted to thermochemical treatment of boro-austempering. The samples were borided at 900 ℃ for 2 and 4 hours, direct cooled from that temperature, and isothermally hold in salt bath at temperatures of Ms –50 ℃, Ms, Ms+50 ℃ for 1 and 3 hours, with subsequent cooling in air to room temperature. The substrate and the layers produced were characterized by optical microscopy (OM), X-ray diffraction (XRD), Vickers microhardness (HRV) and micro adhesive wear tests. The tribological characteristics of the layers were compared with those of the substrate. The micrograph analysis showed the effectiveness of boro-austempering treatment in the production of carbide-free bainite microstructure and the production of boride layers on the surface. As a result, there was a substantial increase in surface wear resistance when compared to the substrate.

Keywords: carbide-free bainite, retained austenite, boro-austempering, wear resistance

Precipitation behavior of Nb in high temperature ferrite

Qiannan Liu, Xuemin Wang, Xiangyu Xu, Dan Liu
(Collaborative Innovation Center of Steel Technology, University of Science and Technology Beijing, Beijing, China)

Abstract: With the rapid development of China's economy and society, the output of steel increases rapidly. In order to develop high-performance and light steel, low-density steel is obtained by adding Al into steel. Aluminum is a ferrite forming element, and the delta ferrite phase region will be enlarged and the austenite phase region will be reduced sharply with the increase of Al content. However, for the Al-baring delta-ferrite steel, the grain refinement can not be achieved by conventional phase transformation. In order to obtain the effect of precipitation strengthening and grain refinement, Nb is added to control the grain refinement. In order to accurately explain the effect of Nb, it is necessary to quantitatively grasp the solid solubility of Nb in steel and the amount of microalloyed carbonitrides formed. We need alculate the solid solubility product of microalloyed carbonitrides in an iron matrix.

The matrix of the steel specimen used in the experiment is ferrite. The samples were dissolved at 1250 ℃ and then heated to 900, 950, 1000, 1050, 1100, 1150, 1200, 1250 ℃, fully insulated, and then quenched rapidly. The content of solid solution Nb under different temperatures was measured by electrolytic phase analysis.

Table 1 is the solid solution data of NbC in ferrite, and its value is calculated by corresponding data. The solubility of NbC in ferrite is obtained by linear regression fitting to the data listed in the table. $\lg([Nb][C]^{0.875})=3.56–8801/T$.

Some researchers have obtained the solubility of NbC in α-Fe by thermodynamics calculation: $\lg([Nb][C]^{0.875})=4.87–10060/T$.

The solid solubility of Nb fitted by this experiment are relatively close to the calculated. The results show that the precipitation of NbC is a little later.

The lattice constant of the matrix increases with the addition of Al, and the misfit between the matrix and the second phase changes, and the interfacial energy can be changed. NbC precipitate with the size of 20-50 nm and the shape of elliptic were observed after specimens were tempered at 900 ℃ for 1h under TEM.

The misfit in the direction of $[hkl]_{NbC}//[h'k'l']_{\alpha}$ can be calculated from the crystal plane relation $(hkl)_{NbC}//(h'k'l')_{\alpha}$. $\delta=\left|\frac{d_{hkl}-d_{h'k'l'}}{d_{hkl}}\right|$, $d_{hkl}=\frac{a}{\sqrt{h^2+k^2+l^2}}$, $a=a_0(1+\alpha)(T-T_0)$.

Among them, d and d' are the interplanar distance of the new phase and the parent phase; a is the lattice constant; a_0 is the lattice constant at room temperature; T_0 is 20 ℃; α is the linear expansion coefficient. The new phase is NbC and the parent phase is ferrite matrix. The lattice constant of the matrix at room temperature was determined by XRD to be 0.2877, and the coefficient of linear expansion measured by thermal simulation is 1.52×10^{-5}. The lattice constant of NbC is 0.4470, the coefficient of linear expansion is 6.5×10^{-6}, and the NbC phase generally has a B-N orientation relationship with the ferrite matrix: $(001)_{NbC}//(001)_{\alpha}$, $[010]_{NbC}//[110]_{\alpha}$.

The misfit between NbC precipitation and ferrite matrix at different temperatures is obtained. The results are shown in Table 2.

In Table 2, δ_2 is the misfit between NbC and ferrite in the direction of $[010]_{NbC}//[110]_{\alpha}$ and $[100]_{NbC}//[1\text{-}10]_{\alpha}$, and its value is between 0.08 and 0.09, belonging to the typical semi-coherent interface with smaller mismatch degree; but the mismatch degree between [001] NbC /[001] A is between 0.35 and 0.37, which is not strictly within the semi-coherent interface range. The ratio of the maximum rotating surface diameter d to its thickness h (i.e. shape factor η) is between 1.63 and 1.65, so the shape of NbC is flake.

The solubility of NbC in ferritic steel obtained by electrolysis is Lg([Nb][C]$^{0.875}$)=3.56–8801/*T*, which is similar to the result calculated by thermodynamic theory, but the precipitation of NbC is later. The lattice constant of steel matrix increases, misfit decreases and shape and size changes with the addition of Al. Elliptical NbC with a diameter of about 50 nm is observed after tempering at 900 ℃.

Keywords: precipitation behavior, Nb, high temperature ferrite

Table 1 Solid solution data of NbC in ferrite

T/℃	Nb(s.s.)/%	Nb(NbC$^{0.875}$)/%	C(s.s.)/%	T^{-1}/ 10^{-4}K^{-1}
900	0.0012	0.0888	0.0135	8.524
950	0.0214	0.0686	0.0161	8.176
1000	0.0341	0.0559	0.0178	7.855
1050	0.0328	0.0572	0.0176	7.558
1100	0.0535	0.0365	0.0203	7.283
1150	0.0640	0.0260	0.0216	7.027
1200	0.0815	0.0085	0.0239	6.788
1250	0.0852	0.0048	0.0135	6.565

Table 2 Mismatch between NbC and ferrite matrix

T/℃	*a*	*a'*	δ_1	$f(\delta_1)$	δ_2	$f(\delta_2)$	η
850	0.44943	0.29049	0.35177	0.35662	0.08326	0.15375	1.660
900	0.44958	0.29071	0.35149	0.35638	0.08287	0.15337	1.662
950	0.44972	0.29093	0.35121	0.35613	0.08248	0.15300	1.664
1000	0.44987	0.29115	0.35094	0.35588	0.08209	0.15262	1.666
1050	0.45001	0.29136	0.35066	0.35563	0.08169	0.15225	1.668
1100	0.45016	0.29158	0.35038	0.35538	0.08130	0.15187	1.670
1150	0.45030	0.29180	0.35011	0.35513	0.08091	0.15149	1.672
1200	0.45045	0.29202	0.34983	0.35489	0.08052	0.15111	1.674

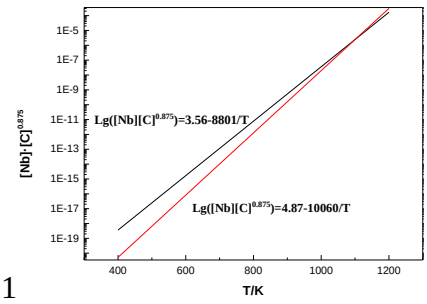

Fig.1

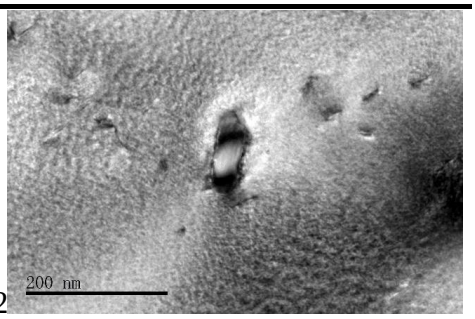

Fig.2

Fig. 1 solid solubility product formula of Nb in ferrite

Fig. 2 precipitation of niobium carbide in ferrite

Microstructure and mechanical properties comparison of one-step and two-step annealing of a medium Mn-TRIP steel

Dapeng Yang
(The State Key Laboratory of Rolling and Automation(RAL) Northeastern University)
yangdapeng6@163.com

Abstract: High-strength steel with good ductility is a vital material for constructing lightweight automobiles, allowing energy conservation, emission reduction and passenger safety. For most materials, the ductility is decreased with increasing strength. The exceptions are the TRIP steels, the strength and ductility can be enhanced simultaneously due to the austenite to martensite transformation during plastic deformation. Medium Mn-TRIP steels containing 5-12wt% of manganese have received a lot of attentions due to their excellent combination of strength and ductility. An austenite reverted transformation (ART) annealing from fresh martensite was adopted to get a lath structure of the mixture of ferrite and Mn-rich austenite due to manganese partition by isotheremal holding for hours, which are only consistence for the batch annealing process in the industry. But the mechanical properties are very sensitive to the isothermal temperatures since the phase fraction and composition of austenite change drastically with the temperature. So that the one-step batch annealing is not suitable for the industrial production of medium Mn steels. The continuous annealing line is being widely used in the heat treatment of steels due to its precisely temperature control, but the manganese partition of medium Mn steels is insufficient during several minutes.

In the present study, a typical medium Mn steel containing the composition of 0.15C-7Mn was hot-rolled and intercritical annealed at a higher temperature for several minutes and followed by a lower annealing for ten hours (two-step annealing), simulating continuous annealing and batch annealing respectively. The microstructure and mechanical properties differences at different batch annealing temperatures was compared to the one-step batch annealing.

Tensile specimens of dimensions 12.5 mm width and a gauge length of 50mm were machined from the annealed sheets with the tensile axis parallel to the rolling direction. Tensile tests were carried out at room temperature at a constant speed of 2 mm $\cdot$min^{-1}. Microstructural was examined using electron microprobe analysis (EMPA) and transmission electron microscope (TEM). The volume fraction of austenite was determined by X-ray diffraction (XRD) with Cu Kα radiation.

The hot-rolled plate of medium Mn steel has a major athermal α′ martensite microstructure due to its good hardenability. After intercritical annealing, a mixed microstructure of lath-shaped ferrite and retained austenite phases were formed due to the austenite reverted transformation and recovery of remaining martensite. After a short-time annealing, a certain volume fraction of lath-shaped austenite was formed due to the partition of C, the rest was lath-shaped ferrite which was alternative distributed to the austenite and the partition of Mn between the two phases was weak. During the following long-time annealing, the austenite grew from the pre-existing austenite by the consumption of ferrite, accompanied by the diffusion of Mn from ferrite to austenite. The hot-rolled and annealed specimens exhibited continuous yielding during tensile testing. Compared to the one-step annealing, the volume fraction and C, Mn content of austenite in the two-step annealing specimens showed a lower temperature sensitivity. As a result, the tensile properties after the two-step annealing such as yield strength, tensile strength and total elongation were relatively stable at a certain temperature range of the second annealing, which was favorable to the industrial production of the medium Mn steels using batch annealing.

Keywords: medium Mn steel, batch annealing, continuous annealing, temperature sensibility

Effect of shell foaming agent on physical properties of AlSi7Mg alloy closed cell foam

Junwen Li, Xiang Ma, Chufeng Shan, Yingli Teng
(Dalian Jiaotong University)
joelee0527@163.com

Abstract: Metallic foams are commonly produced using hydride and carbonates foaming agents. However, carbonate foaming agents are safer to handle than hydrides and produce aluminum foam with a fine, homogenous cell structure, low cost and easily available. The number of pores per inch and relative density of the foam play an important role on their physical and mechanical properties. Hence it is very important to investigate effect of particle size of shell foaming agent on pores per inch and relative density. The present work deals with the effect of particle size of the shell forming agent on the physical properties of a eutectic Al-Si alloy closed cell foam. The foam was produced with different particle size of shell (150, 106, 75, 53 μm) as a foaming agent. The pores per inch and density of the foam produced with different particle size of shells as foaming agent are determined. Relative density is in the range of 0.21-0.34, pores per inch are in the range of 11-20 for the produced AlSi7Mg alloy closed cell foam. It is observed that as particle size of shell used for production of aluminum foam increases, the number of pores per inch decreases, relative density decreases and porosity increases.

Keywords: aluminum foam, shells, foaming process, relative density

FEM simulation of new tailored hot forming process for high strength steel

Tao Yang, Xianjun Li, Junqing Hou, Xiaolin Wu, Ping Luo, Ruijie Xi
(Beijing Research Institute of Mechanical and Electrical Technology)
imlixj@163.com

Abstract: The tailored hot forming process can achieve specific mechanical properties in different areas of high-strength steel sheet, thereby improving the comprehensive service performance of the hot forming parts, to better meet the requirements of automotive lightweight and the crashworthiness of car collision. This paper briefly introduces the tailored hot forming process such as tailored weld blank and performance gradient distribution mold etc. A new type of tailored hot forming process is studied in this paper. That is, when the steel sheet is heated to 950 ℃ in the furnace, it enters the temperature controlling mechanism, and adopts the fast cooling technology to make the tailored area cool down to a certain temperature and then hot stamping to achieve the tailored strength requirement. This paper mainly simulates the process of rapid cooling of tailored area. A numerical model of steel plate cooling is established, and the parameters of rapid cooling for different thickness steel plates are determined, which is of guiding significance for the design of new tailored hot forming process.

Keywords: tailored hot forming, rapid cooling, numerical simulation

Research and development of ultra-high strength steel in hot stamping technology

Xiao Liang, Xianjun Li, Huasheng Xie
(Beijing Research Institute of Mechanical andElectrical Technology)
liangxiao@jds.ac.cn

Abstract: Hot stamping technology is widely used in the manufacture of automotive parts. Boron steel as ultra-high strength steel is mainly used for automotive structure parts. As one of typical boron steel in hot stamping has good forming performance and high strength. The research and development of boron steel in hot stamping, the microstructure evolution and mechanism of enhancement of (Nb-Ti, Ti) micro-alloy hot stamping boron steel and the resent research progress on the coating technology (Al-10Si, GI/GA, Zn-10Ni) were introduced. Combined with the hot stamping technology, the research progresses of flow behaviors and forming limit at elevated temperatures and the microstructure evolution process of hot stamping parts were investigated.

Keywords: hot stamping, ultra-high strength steel, micro-alloy, coating technology, microstructure evolution

Cavitation degassing of commercially pure copper melt during solidification

Junwen Li
(Dalian Jiaotong University)

Abstract: The effect of high intensity ultrasonic vibration (UV) on degassing of pure copper has been studied in this paper. The methods of reduced pressure test (RPT) and direct hydrogen and oxygen measurements are used for the evaluation of degassing efficiency on hydrogen and oxygen concentrations. The results showed that high intensity UV had a significant degassing effect for the commercially pure copper (CP-Cu) melt. With UV, the density index Di was reduced from 11.94 to 1.13%, and the product of hydrogen-oxygen concentration ([%H][%O]) in the liquid Cu was decreased to 1.44010-5 from 6.62410-5. It was also found that electric power and ultrasonic treatment time could influence the degassing efficiency.

Keywords: solidification, cavitation

On-line spheroidization behavior and microstructure evolution of non-annealed cold heading steel SWRCH35KM

Leyu Zhou
(Beijing Research Institute of Mechanical & Electrical Technology)
zhouleyu@ustb.edu.cn

Abstract: Mechanical simulation experiment of non-annealed cold heading steel SWRCH35KM was carried out on Gleeble1500 thermal simulator to research continuous cooling transformation rule and on-line spheroidized behavior of pearlite. Microstructure evolution of on-line softening was investigated. Ferrite and pearlite have transformed in cooling rate range of 0.1-25 ℃/s. The critical cooling rate of spheroidization behavior is lower than 0.2 ℃/s. When the cooling rate is over 2 ℃/s, there is acicular ferrite and Widmannstatten. During the slow cooling process after compression at 850-750 ℃, the key temperature range of pearlite spheroidization is about 660-630 ℃. Decreasing of deformation temperature induce the appearance of spheroidized pearlite. Spheroidization phenomenon take place at fine pearlite colony and edge of coarse pearlite colony.

Keywords: Non-annealed cold heading steel, on-line spheroidized of pearlite, microstructure evolution